



# Sensitivity assessment of hydrologic processes in an eastern Himalayan watershed to potential climate change using RHESSYS

Pooja Mishra<sup>1</sup> · Arnab Bandyopadhyay<sup>1</sup> · Aditi Bhadra<sup>1</sup>

Received: 24 November 2021 / Accepted: 16 May 2023 / Published online: 25 May 2023  
© The Author(s), under exclusive licence to Springer Nature Switzerland AG 2023

## Abstract

Climate changes are likely to significantly affect the region's hydrological cycle, as any change in hydrological variables disturbs the hydrologic processes. In the present study, the Regional Hydro-Ecological Simulation System (RHESSys) was set up in the Nuranang watershed located in the Tawang district of Arunachal Pradesh, India, to explore the sensitivity of the hydrologic response of the watershed toward the projected future climatic scenarios. Future streamflow and saturation deficit were obtained by driving the calibrated RHESSys model and Coupled Model Intercomparison Project Phase 5 (CMIP5) climate data downloaded from the COordinated Regional Climate Downscaling Experiment-South Asia (CORDEX-SA) website (<ftp://cccr.tropmet.res.in/>) under Representative Concentration Pathways (RCPs) 4.5 and 8.5 scenarios. All the Global Climate Models (GCMs) predicted that the study region's average temperature would rise by 1.39–6.39 °C in the twenty-first century compared to the baseline period. All models projected a higher temperature increase under RCP 8.5 than under RCP 4.5. The model-average total precipitation increased in the 2020s but decreased in the 2050s and 2080s under both RCP scenarios. Monthly, the projections show a prevalent summertime drying (while the winter experiences higher precipitation). Changes in subsurface flow, overland flow, and streamflow followed almost the same trend as changes in precipitation. RCP 4.5 scenario predicts about 1.97% increase in total streamflow in 2020s and a deficit of about 0.60% and 3.54% in 2050s and 2080s, respectively, as compared to baseline period and under RCP 8.5 scenario the model-average predicted streamflow increased by 2.26% in 2020s and reduced by around 1.81% and 2.34% in 2050s and 2080s respectively. On a monthly scale, total streamflow increased significantly in winter and decreased in summer for all projected time slices. The model-average saturation deficit decreased in all future time slices as compared to the baseline period, except in the 2020s under RCP 4.5. Overland flow and streamflow were found most sensitive to climate change under the RCP 4.5 scenario, whereas saturation deficit and overland flow were found most sensitive under the RCP 8.5 scenario.

**Keywords** Climate change · CMIP5 · CORDEX · Hydrological processes · RCP

## Introduction

Increases in the concentrations of greenhouse gases in the atmosphere are expected to affect the Earth's climate in the coming century, significantly affecting the hydrological cycle. Changes in climatic variables like temperature and precipitation disturb the hydrological cycle and water availability. Planning and management of water resources are essential for the region's environment, ecosystem, and

economic development. Climate variables and, accordingly, the pattern of streamflow are highly variable both inter-annually and intra-annually. Hydrological models with assumed climate change scenarios are generally used to evaluate the possible effects of climate change on water resources and hydrological processes. The projection of future flow regimes and water availability in the watershed can be beneficial for the adaptation of water resources management strategies and the socio-economic development of the region (Ruth et al. 2007; Fung et al. 2013).

All the major rivers of India originating in the Himalayas can be affected by climate change as rainfall, snow, and glacier melt contribute to runoff. Studying on climate change's influence on the flow regime of river systems helps in the planning and management of water resources, disaster

✉ Arnab Bandyopadhyay  
arnabbandy@yahoo.co.in

<sup>1</sup> Department of Agricultural Engineering, North Eastern Regional Institute of Science and Technology, Nirjuli, Arunachal Pradesh 791109, India

management, hydropower generation, etc. In the high altitude regions of the eastern Himalayas, a significant part of the annual precipitation falls as snow; therefore, due to an increase in temperature, precipitation may fall as rain instead of snow and thus disturb the flow regime. Incorporating climate change forecasts (e.g., air temperature and precipitation) into models that accurately estimate water flows in a watershed might help examine climate change's implications on water resources. The most common approach to study hydrological response to climate change is to run hydrological models with projected climate variables (precipitation and temperature) from Global Climate Models (GCMs) under different climatic scenarios generally downscaled or bias-corrected to the study region (Etchevers et al. 2002; Fowler et al. 2007; Chiew et al. 2009; Senatore et al. 2011; Ruelland et al. 2012). GCMs provide climate variation at the continental and hemispheric scales and are naturally unable to represent local basin-scale characteristics. The COordinated Regional Climate Downscaling EXperiment (CORDEX) was launched by the World Climate Research Programme (WCRP) to downscale the Coupled Model Inter-comparison Project Phase 5 (CMIP5) scenarios globally (Giorgi et al. 2009). Among the several CORDEX domains, the South-Asia (SA) domain is a capacity-building effort in the South-Asian region that focuses on the South-Asian summer to translate regional climate downscaled data into meaningful, sustainable development information. CORDEX-SA was started in 2012, and the Regional Climate Model (RCM) outputs of future projections for the South-Asian region are available for some models only (Pechlivanidis et al. 2014).

Distributed watershed scale models have been used increasingly to obtain the streamflow from the watershed and estimate climate change impacts on streamflow (Hussen et al. 2018; Aawar and Khare 2020; Tarekegn et al. 2021). Such models have been utilized in hydrological simulations under numerous situations, including land use and climate change. The impact of climate change on hydrology is studied by comparing the current streamflow at the catchment outlet with the future projected stream flow from two RCPs (RCP 4.5 and RCP 8.5) simulated by different climate models (Beaulieu et al. 2016; Shiferaw et al. 2018; Dutta et al. 2020; Thiha et al. 2020).

The Regional Hydro-Ecological Simulation System (RHESys), a daily time-step distributed hydro-ecologic model, has been used in the present study to derive streamflow and other hydrological variables for the present climate (using climate input for the present condition) as well as for future time periods (using climatic input from climate models) and to investigate the sensitivity of different variables to climate change. RHESys has been successfully applied in various mountainous watersheds to study the climate change impact on the hydro-ecological systems of the watershed (Band et al. 1996; Morán-Tejeda et al. 2015;

Peng et al. 2015; Martin et al. 2017; Sarkar et al. 2018). Zabalza-Martínez et al. 2018 evaluated the response of streamflow in a Mediterranean medium-scale basin under land-use and climate change scenarios. Results reveal a clear decrease in dam inflow (−34%) since the dam was operational from 1971 to 2013. The simulations obtained with RHESys displayed a similar decrease (−31%) from 2021 to 2050. Son and Tague (2018) investigated the effect of climate warming (2 and 4 °C) on the model estimates of snow water equivalent (SWE), streamflow, evapotranspiration (ET), and moisture deficit in the two watersheds in the California Sierra. Shin et al. (2019) examined the effects of climate change on hydrological and ecological variables by applying the RHESys model to the Seolmacheon catchment. The RHESys model previously calibrated and validated for Nuranang watershed using spatial and climatic data (Mishra et al. 2020) was used for future streamflow simulations. Future streamflow and other hydrologic variables were obtained by driving the calibrated RHESys model with climate data from CMIP5 for RCP 4.5 and 8.5.

The hydrological systems of the Himalayan region are very sensitive to changes in the climate. The fluctuations in precipitation and temperature greatly affect the streamflow regime and timing of peaks, which can directly influence the biodiversity and ecosystem. There has been widespread worry among researchers in this region as the effects of climate change on the region's mountain range become more apparent. Changing precipitation and glacier depletion will significantly affect streamflow (Marazi and Romshoo 2018; Rani and Sreekesh 2019; Singh et al. 2021; Thapa et al. 2021; Singh and Sharma 2022). Romshoo and Marazi (2022) studied the influence of shifting precipitation and snowmelt on streamflow in the Lidder, the most glaciated watershed in the Upper Indus Basin (UIB). Climate change predicts early spring snowmelt by the end of the century, altering streamflow peaks from late spring to early spring upstream and from summer to spring downstream. Munawar et al. (2022) examined climatic and hydrological trends in the Jhelum river basin for the twenty-first century using Statistical Downscaling Model (SDSM) and Snowmelt Run-off Model (SRM). According to the study, the twenty-first century will be wetter and warmer than the baseline period. Dar et al. (2022) examined the influence of the cryosphere on streamflow to land system dynamic changes in the Kashmir Himalayan Upper Jhelum River Basin (UJRB). Between 1980 and 2016, temperatures rose, and precipitation fell; and in glacierized sub-basins, snow covered area (SCA) decreased. Since 1998, the average annual discharge also declined.

Studies related to the sensitivity of the hydrologic response of watersheds in the eastern Himalayas are limited. However, the hydrological systems of the region are highly sensitive to change and variability in climatic variables. The

changes in precipitation and temperature greatly influence the streamflow pattern, as the region has a great share of runoff from snowmelt. There is a need to project seasonal streamflow and hydrological property variations at the local scale to build adaptive resource management and hazard alleviation techniques. Therefore, the present study was undertaken to analyze the impact of future climate changes on total streamflow and saturation deficit in the Nuranang watershed of Arunachal Pradesh under different projected climatic scenarios.

This study was conceptualized in 2015 and was completed in 2021 and hence, CORDEX-SA CMIP5 models were used for future projections. However, in May 2021, CORDEX-SA CMIP6 model projections became available, which might give improved insights as per Intergovernmental Panel on Climate Change (IPCC) 6th Assessment Report scenarios.

## Study area

Nuranang watershed (Fig. 1a), draining an area of 52.37 km<sup>2</sup>, located in the Tawang district of Arunachal Pradesh, India, was selected as the study area. The area lies between North latitudes of 27° 29' 57.37"–27° 34' 21.15" and East longitudes of 92° 00' 33.98"–92° 07' 08.93" with an elevation range of 3459 to 4895 m above MSL. The discharge site of the Central Water Commission (CWC) at RA-III, Jang, was selected as the outlet point at 27° 33' 00" N and 92° 01' 19" E, with an elevation of 3459 m above MSL. The entire watershed receives seasonal snowfall from October until

March, and depletion starts in February and continues until early June, when snow completely depletes. Snow accumulation and ablation patterns vary a little year-to-year.

## Methods and data collection

Digital Elevation Model (DEM) with 30 m spatial resolution was downloaded for the study area from the United State Geological Survey (USGS) Earth Explorer (Fig. 1a). Land Use/Land Cover map for the state of Arunachal Pradesh was purchased from the State Remote Sensing Application Centre (SRSAC), Department of Science and Technology, Govt. of Arunachal Pradesh (Fig. 1b). The hydrological data of daily discharge and daily stage for the Nuranang watershed for 1999–2011, measured at the CWC discharge site at RA-III, Jang, were collected from the CWC office, Itanagar, Arunachal Pradesh. The observed stage for the year 2016 was taken from the Digital Water Level Recorder (DWLR) installed at the outlet of the Nuranang catchment purchased from Virtual Hydromet, Roorkee, India (<http://www.vhydr.com/>). Daily precipitation, maximum temperature, and minimum temperature data for the present condition (1970–2005) and future years (2006–2097) under RCP 4.5 and RCP 8.5 scenarios for different CMIP5 (Coupled Model Intercomparison Project Phase 5) models were downloaded from the CORDEX-SA website (<ftp://cccr.tropmet.res.in/>). Five GCMs (ACCESS 1.0, CCSM 4, CNRM-CM5, MPI-ESM-LR, NorESMI-M) for which CORDEX output were available for both present and future years were selected. Daily CORDEX-SA data for all GCMs are available at 0.5° × 0.5° spatial resolution.

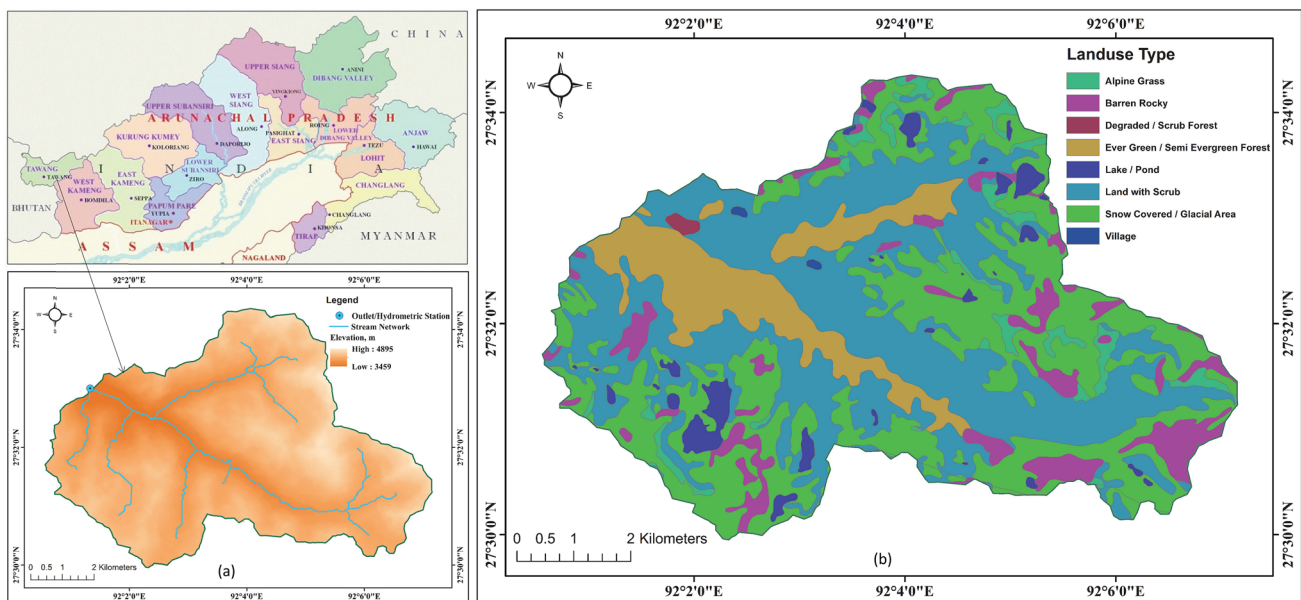


**Fig. 1** Nuranang watershed, Arunachal Pradesh, India: **a** DEM and **b** LULC map

## Pre-processing of CORDEX-SA data

The downloaded CORDEX data were in numerical control file format (.nc); the data were converted to GeoTIFF format using QGIS software. The resultant raster images were then clipped for the watershed shapefile using ArcMap 10.0. The extraction of time series for temperatures (maximum and minimum) and precipitation was also done using the Spatial Analyst tool in ArcMap 10.0. The time series data obtained from the above process were exported to Microsoft Excel for further analysis.

## Generation of rating curve for Nuranang watershed

A rating curve (stage-discharge curve) was needed in this study to convert the daily stage (m) data recorded by the DWLR installed at the watershed outlet into discharge ( $\text{m}^3 \text{s}^{-1}$ ) for the year 2016. These observed streamflow data were used to validate the projected streamflow generated by the RHESSys simulation under projected climate (temperature and precipitation) forcings. The time series data of the stage (m) at the outlet and the corresponding discharge ( $\text{m}^3 \text{s}^{-1}$ ) from the watershed from 2000 to 2011 were arranged in ascending order. On the corresponding scatter plot, it was observed that the data points are organized in a straight line since the stream is small and the catchment size is only about 52 sq. km. Hence, the best-fit

straight line through these data points was drawn by linear regression, and the corresponding linear equation was obtained as the rating curve equation for future use. Ninety percent of the available data points were used in developing the equation, and the remaining 10% of randomly selected data points were used to validate the developed rating curve.

Figure 2a shows the developed stage-discharge rating curve of the Nuranang watershed at the CWC gaging site at RA-III, Jang, and the regression analysis gave the best fit linear equation as:

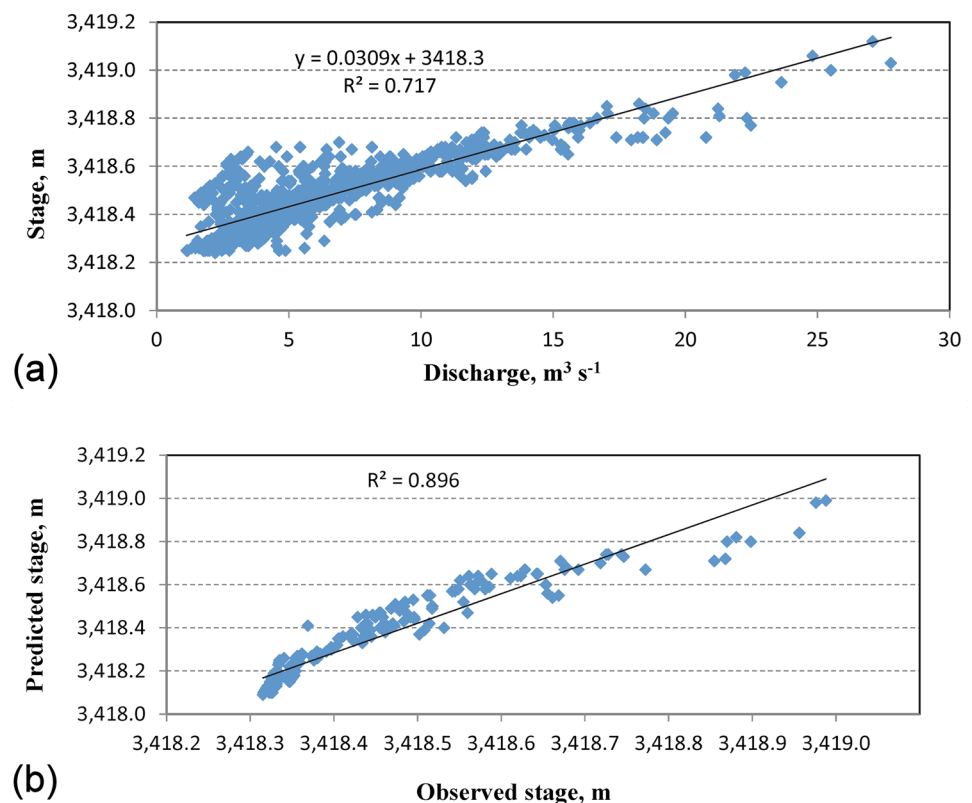
$$Y = 0.0309X + 3418.3, \quad (1)$$

where,  $Y$  is the observed stage (m) and  $X$  is the observed discharge ( $\text{m}^3 \text{s}^{-1}$ )

The coefficient of determination ( $R^2$ ) of the equation was found to be 0.717.

The generated rating curve equation was validated for data points not used in the generation process. The data points for the validation process were randomly selected in such a way that the range covered both low and high flows. Figure 2b shows the plot of the predicted/ estimated stages using the developed rating curve equation vs. the observed stages. Five dimensionless statistical performance criteria, namely, NSE (Nash–Sutcliffe efficiency), KGE (Kling–Gupta Efficiency), CRM (Coefficient of Residual Mass),

**Fig. 2** Rating curve for Nuranang watershed: **a** development, **b** validation



$R^2$  (Coefficient of Determination), and SEE (Standard Error of Estimates), were used for validation. Simulated stage values showed a high level of agreement with the observations, with NSE and KGE of 0.81 and 0.84, respectively. The  $R^2$  value obtained for validation was 0.896. The corresponding CRM and SEE values obtained were  $-0.001$  and  $0.074$ , respectively, indicating slight overestimation. Therefore, the developed equation was used to convert the DWLR recorded daily stage data of the year 2016 to the corresponding discharge for further use.

## RHESSys

RHESSys is a distributed physical processes-based eco-hydrological model developed by coupling ecological and hydrological models (Band et al. 1993; Tague and Band 2004). Originally, the RHESSys model was designed by explicitly coupling the Forest Biogeochemical Cycles (FOREST-BGC) canopy model with a Mountain Climate Simulator (MT-CLIM) and advanced by coupling with topography based hydrological model (TOPMODEL) for the hydrologic process. RHESSys is capable of simulating

water, carbon, and the nitrogen cycle in a forest-dominated basin using a geographical information system. The Forest-BGC model simulates the vegetation growth, nutrient, and water cycle of the forest ecosystem while MT-CLIM mainly interpolates meteorological variables at a climate station. TOPMODEL (Beven and Kirkby 1979) is a physical-based quasi-distributed hydrological model that generates streamflow and saturation deficits. In addition to streamflow, the model also gives estimates of overland and subsurface flow and the spatial pattern of the depth to the water table in the watershed. For an advance in hydrological processes, an explicit hydrologic routing model, the Distributed Hydrology Soil Vegetation Model (DHSVM), was incorporated in RHESSys to account for non-grid-based patches and non-exponential transmissivity profiles. Model developers (Band et al. 1993; Tague and Band 2004) have described more details on each module and algorithm of RHESSys.

The RHESSys model was used to assess how climate changes might impact future streamflow regimes. The RHESSys model, driven by historical precipitation, minimum and maximum air temperature data, was first calibrated and validated using daily streamflows at the watershed

**Fig. 3** Estimation of effect of climate change on hydrological variables using RHESSys

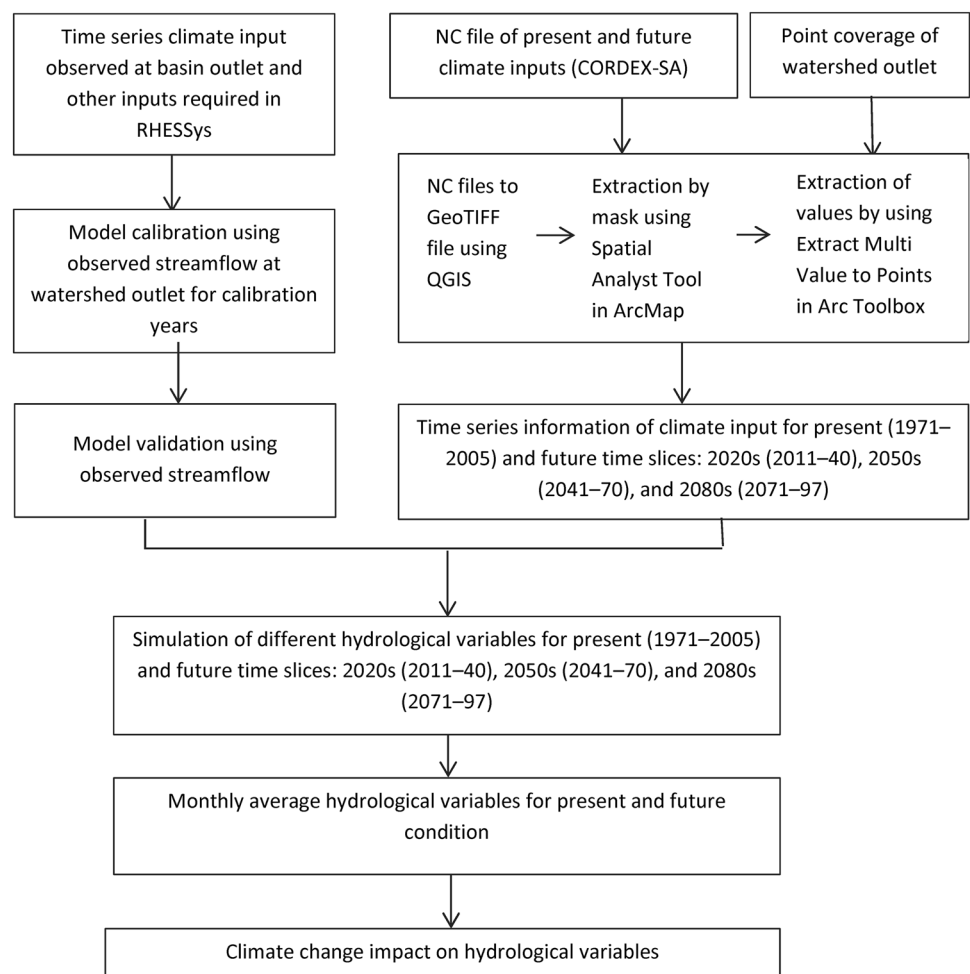
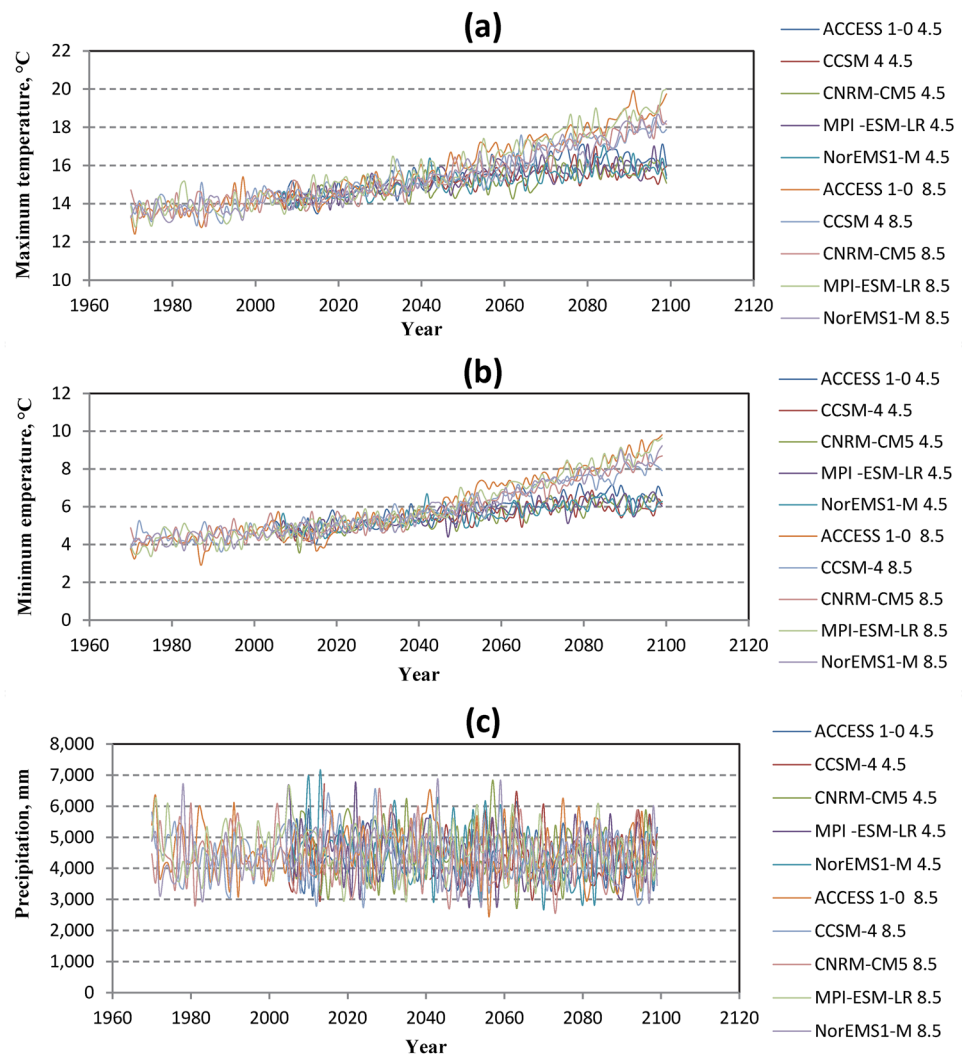




**Fig. 4** Yearly average climatic variables projected by different GCMs: **a** maximum temperature, **b** minimum temperature, **c** total precipitation



outlet. Future streamflow was then obtained by driving the calibrated RHESSys model with daily scenarios of different climate data from CMIP5 to examine streamflow regime change sensitivity.

### Governing equations of RHESSys

RHESSys uses TOPMODEL (Beven and Kirkby 1979) to calculate total streamflow from patches and the basin outlet. The model generates streamflow using the variable-source-area concept. Model projections include streamflow, overland flow, subsurface flow, and water table depth in the watershed. TOPMODEL assumes saturated hydraulic conductivity changes exponentially with depth, water table gradients may be represented by topographic slope, and steady-state flow is obtained within the modeling time step. Wolock (1993) and Tauge and Band (2004) provide a detailed overview of the mechanisms employed in RHESSys streamflow generation.

The RHESSys explicit routing model is based on the DHSVM routing technique (Wigmosta et al. 1994), which has been modified to accommodate non-grid-based patches and non-exponential transmissivity profiles. Surface flow (i.e., saturation overland flow or Hortonian overland flow) produced is routed following the same patch topology used for routing saturated subsurface throughflow. All surface flow produced by a patch is assumed to exit from the patch within a single time step. If the receiving patch is not saturated, surface flow is allowed to infiltrate and is added to the unsaturated soil moisture storage. Patch routing is sequenced to start from the uppermost patches in the watershed.

### Future climatic projections

GCMs are tools that enable us to investigate the climate behavior under various forcings and project the future climate over the twenty-first century. Different climate

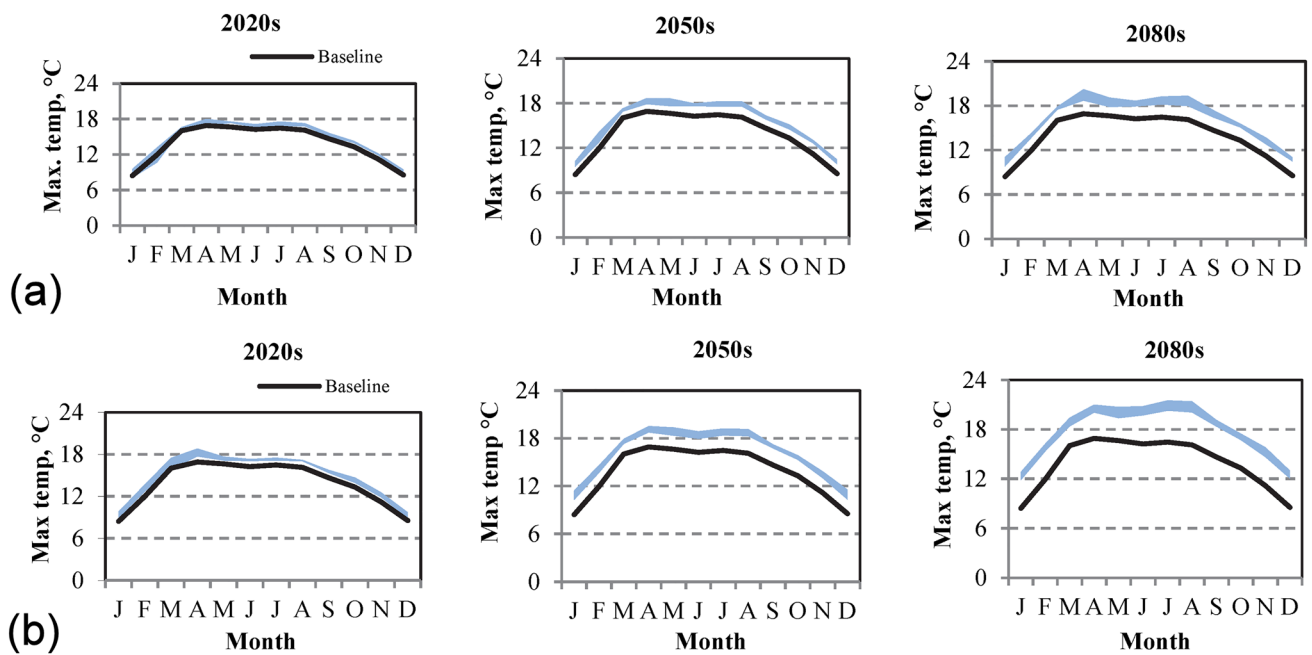


**Fig. 5** Projected maximum temperature ranges under: **a** RCP 4.5 scenario, **b** RCP 8.5 scenario

projection models are available, through which different emission scenarios for different projected future years can be obtained.

### Change in temperature and precipitation

Daily precipitation and maximum and minimum temperatures for present and future years for all five selected models were analyzed to determine the change in them in future years, as compared to the present climatic condition. The available CORDEX data from 1979 to 2097 were divided into four time slices, i.e., the baseline period (1979–2005), 2020s (2011–2040), 2050s (2041–2070), and the 2080s (2071–2097) for both RCP 4.5 and RCP 8.5 scenarios. Daily values of each climate input were averaged to obtain one dataset for each time slice for all five climate models. Daily precipitation for each month was added to obtain monthly precipitation for each climate model for all four time slices. Daily maximum and minimum temperatures were averaged to obtain monthly maximum and minimum temperatures for present and future time slices. Percent changes in each climate variable for each model were estimated compared to the baseline period. The annual percentage change of the climatic variables was also analyzed.

### Impact of climate change on various hydrological variables

The impact of climate change on various RHESSys outputs was evaluated using projected climate forcings from

CORDEX-SA for future years under RCP 4.5 and RCP 8.5 scenarios (Fig. 3).

Daily maximum and minimum temperatures and precipitation data for the present climate (1979–2005) and future years (2006–2097) were used as climate forcings in the RHESSys model. The RHESSys model was run for three future time slices (2020s, 2050s, and 2080s) and for the baseline period to analyze the change in hydrological and ecological variables as compared to the present climate. RHESSys outputs for baseline and future periods under RCP 4.5 and RCP 8.5 scenarios for each climate model were compared to evaluate the impact of climate change on different hydrological variables.

### Sensitive hydrological variables to climate change

In the present work, hydrological sensitivities were measured as the percentage change in hydrological variables with changes in climatic inputs (maximum temperature, minimum temperature, and precipitation) as compared to the baseline period. The Sensitivity of different hydrological variables to climate change was estimated by comparing the RHESSys outputs for the baseline period (present climate condition) with the future periods for all five climate models under the RCP 4.5 and RCP 8.5 scenarios. The percent change in each variable in future periods as compared to the baseline period was obtained under both the scenarios (RCP 4.5 and RCP 8.5) of all five climate models for the future periods of the 2020s, 2050s, and 2080s. The average percentage change in each variable for each month as compared to the baseline

**Table 1** Monthly changes in average maximum temperature (°C) under different RCP scenarios

Mon	Baseline	RCP 4.5/RCP 4.5						RCP 8.5					
		2020s		2050s		2080s		2020		2050		2080	
		Avg value	Change	Avg value	Change	Avg value	Change	Avg value	Change	Avg value	Change	Avg value	Change
Jan	8.43	0.72	9.94	1.51	10.43	2.00	9.44	1.02	10.79	2.36	12.38	3.95	
Feb	11.94	0.37	13.32	1.38	14.02	2.08	12.93	0.99	14.19	2.25	15.74	3.79	
Mar	16.03	0.38	17.17	1.14	17.63	1.60	16.64	0.61	17.63	1.60	19.08	3.05	
Apr	16.92	0.67	18.38	1.46	19.15	2.23	17.95	1.03	19.06	2.14	20.56	3.64	
May	16.64	0.81	18.01	1.37	18.40	1.76	17.44	0.81	18.69	2.05	20.04	3.40	
Jun	16.24	0.68	17.75	1.51	18.16	1.92	17.15	0.91	18.33	2.09	20.17	3.93	
Jul	16.46	0.74	17.87	1.41	18.62	2.15	17.34	0.87	18.70	2.24	20.78	4.31	
Aug	16.13	0.87	17.87	1.75	18.53	2.40	17.09	0.96	18.61	2.48	20.66	4.53	
Sep	14.65	0.67	16.14	1.49	16.73	2.09	15.57	0.93	16.97	2.32	18.76	4.12	
Oct	13.30	0.79	14.86	1.55	15.33	2.02	14.32	1.02	15.58	2.28	17.08	3.78	
Nov	11.17	0.80	12.87	1.70	13.12	1.94	12.08	0.91	13.39	2.22	15.24	4.07	
Dec	8.53	0.71	10.23	1.70	10.66	2.13	9.32	0.79	10.78	2.25	12.50	3.97	
Avg		0.68	10.23	1.50	10.66	2.03	9.32	0.90	10.78	2.19	12.50	3.88	

period was calculated. Different variables were ranked as per their sensitivity to climate change (based on percentage change as compared to the baseline period).

**Comparison of climate projected streamflow with observed streamflow**

The projected streamflow using RHESys model was compared with the observed streamflow measured using the DWLR at the outlet of the watershed to validate the future projection of streamflow generated using RHESys and climatic models. Total streamflow for the depletion period of 2016, i.e., from 01-04-2016 to 30-09-2016, was generated by RHESys simulation with climate forcings from CMIP5 (ACCESS 1.0, CCSM 4, CNRM-CM5, MPI-ESM-LR, and NorESM1-M) projected future precipitation, maximum temperature, and minimum temperature under RCP 4.5 and RCP 8.5 scenarios.

The observed streamflow at the outlet of the watershed was obtained from the stage data recorded at the outlet using the DWLR. The developed rating curve (Eq. 1) for the Nuranang watershed was used to convert the observed stage to the observed discharge. The total discharge observed during the depletion period of the year 2016 was compared with the simulated discharge using future climate data from CORDEX to validate the projected streamflow using RHESys coupled with climatic models.

**Results and discussion**

**Model testing**

To evaluate the applicability of the RHESys model in Nuranang watershed, the model was calibrated and validated using the required meteorological (temperature and precipitation) data and spatial inputs (DEM, soil map, vegetation map) of the watershed. The model was successfully calibrated for the years 2004 and 2005 and validated for the years 2008 and 2009 using observed daily streamflow at the watershed outlet. Magnitude, evolution, and variation of streamflow were well reproduced in both calibration years. The RHESys simulated streamflow matched daily observed discharge well with model efficiency (ME) of 0.75 and 0.82 for calibration years 2004 and 2005, respectively. For the validation year also, simulated streamflows showed a high level of agreement against observed streamflow, with ME values of 0.74 and 0.77 for the years 2008 and 2009, respectively (Mishra et al. 2020).



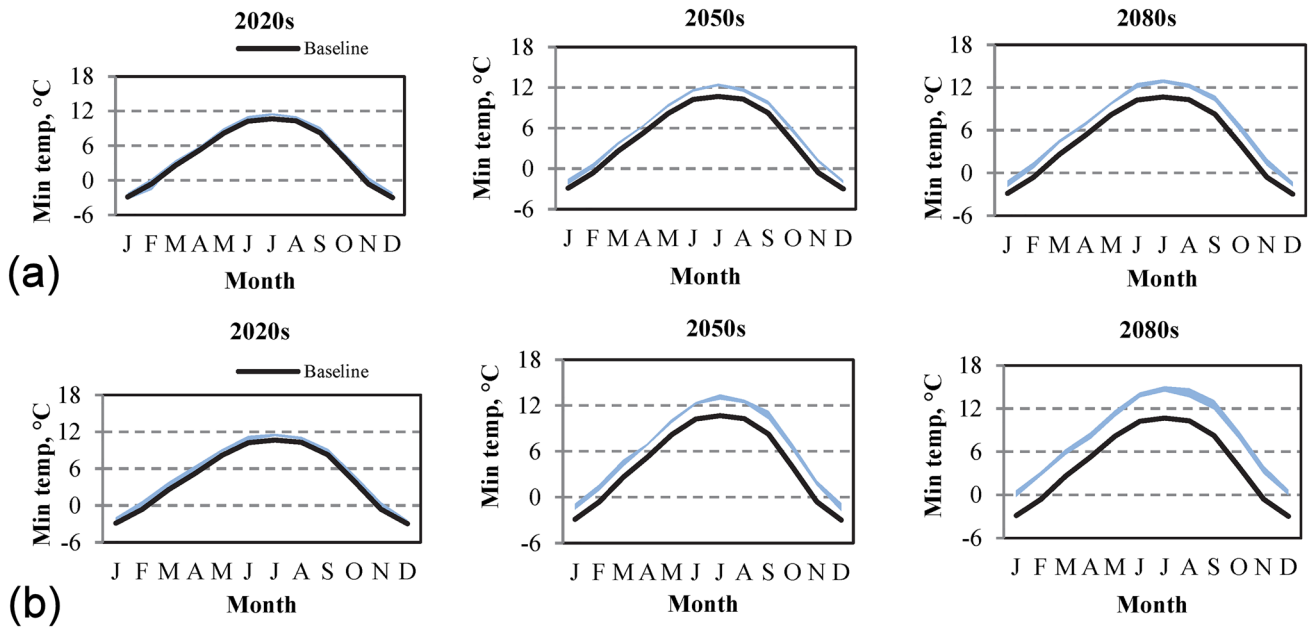


Fig. 6 Projected minimum temperature ranges under: a RCP 4.5 scenario, b RCP 8.5 scenario

Table 2 Monthly changes in average minimum temperature (°C) under different RCP scenarios

Mon	Baseline	RCP 4.5						RCP 8.5					
		2020s		2050s		2080s		2020		2050		2080	
		Avg value	Change	Avg value	Change	Avg value	Change	Avg value	Change	Avg value	Change	Avg value	Change
Jan	-2.89	-2.54	0.35	-2.00	0.89	-1.57	1.32	-2.30	0.59	-1.24	1.65	0.24	3.13
Feb	-0.62	-0.36	0.26	0.42	1.04	1.08	1.70	0.12	0.74	1.31	1.93	2.92	3.54
Mar	2.60	3.18	0.58	3.76	1.16	4.37	1.77	3.42	0.82	4.44	1.84	5.95	3.35
Apr	5.25	5.83	0.58	6.30	1.05	6.79	1.54	6.09	0.83	6.90	1.65	8.15	2.90
May	8.16	8.68	0.52	9.30	1.14	9.74	1.58	8.93	0.76	10.02	1.86	11.33	3.17
Jun	10.23	10.75	0.51	11.57	1.34	12.31	2.08	10.94	0.71	12.28	2.05	13.85	3.62
Jul	10.68	11.41	0.73	12.35	1.67	12.91	2.23	11.48	0.80	13.06	2.38	14.74	4.06
Aug	10.28	10.93	0.65	11.62	1.34	12.21	1.93	10.92	0.64	12.45	2.17	14.15	3.87
Sep	8.24	8.86	0.61	9.76	1.52	10.41	2.16	8.96	0.72	10.57	2.33	12.39	4.15
Oct	3.92	4.52	0.61	5.56	1.64	6.04	2.13	4.72	0.80	6.49	2.57	8.13	4.21
Nov	-0.60	0.08	0.69	1.09	1.70	1.42	2.03	0.18	0.78	1.79	2.40	3.47	4.08
Dec	-2.98	-2.46	0.52	-1.91	1.06	-1.59	1.38	-2.60	0.38	-1.31	1.67	0.30	3.27
<b>Avg</b>			0.55		1.30		1.82		0.71		2.04		3.61

**Future climate projection**

**Yearly average temperature and precipitation**

The maximum temperature and minimum temperature obtained from each GCM for each year were averaged to obtain yearly average maximum and minimum temperatures in baseline and future periods (Fig. 4a, b). Temperature changes were similar in both scenarios (RCP 4.5 and RCP

8.5), but the amplitude was significantly higher in RCP 8.5. The increase in maximum temperature (Fig. 4a), i.e., the difference between 1970 and 2097, was maximum for ACCESS 1.0 (2.67 °C under RCP 4.5 and 6.39 °C under RCP 8.5) and minimum for CCSM 4 (2.00 °C under RCP 4.5 and 3.92 °C under RCP 8.5). The minimum temperature (Fig. 4b) also increased in future years under both RCP 4.5 and RCP 8.5 scenarios. The increase in minimum temperature was also maximum for ACCESS 1.0 (2.80 °C under RCP 4.5 and

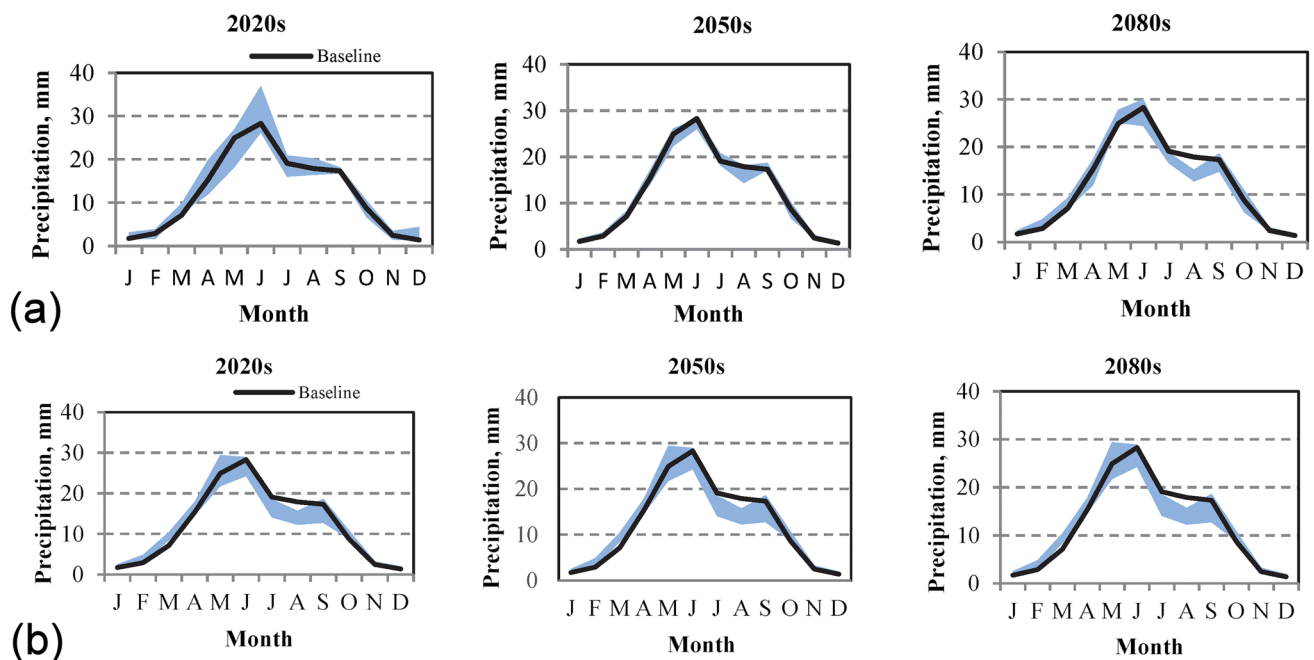


**Fig. 7** Projected precipitation ranges under: **a** RCP 4.5 scenario, **b** RCP 8.5 scenario

6.02 °C under RCP 8.5) and minimum for CCSM 4 (1.39 °C under RCP 4.5 and 3.81 °C under RCP 8.5).

All five GCMs indicated that the study region would be warmer in the twenty-first century, with average temperature increasing between 1.39 and 6.39 °C depending on the climate model and scenario considered, which agreed well with the climate change study in the western Himalayas by Tiwari et al. 2018 who reported temperature increases of 1.5–5.0 °C in all the seasons. The increase in temperature was also quite comparable with the study of Urrutia and Vuille (2009) in tropical South America, where the temperature was estimated to increase between 2 and 7 °C in 2100, depending on the location and scenario considered. Total precipitation did not follow any specific temporal trend in the baseline and future periods (1970–2097) under RCP 4.5 and RCP 8.5 for five GCMs (Fig. 4c).

### Maximum temperature envelope under projected climatic scenarios

The average maximum temperature was observed at its minimum in January, then gradually increased to April, decreased a little in May–June, increased again in July–August, and finally decreased up to December in the baseline period as well as in all three future time slices under both RCP 4.5 and 8.5 scenarios (Fig. 5 and Table 1).

Under the RCP 4.5 scenario, the average maximum temperature was observed maximum in April (17.59 °C in the 2020s, 18.38 °C in the 2050s, and 19.15 °C in the 2080s)

and minimum in January (9.15 °C in the 2020s, 9.94 °C in the 2050s, and 10.43 °C in the 2080s) in all the three future time slices (Table 1). The average maximum temperature was projected to increase for all the months in all future time slices. Model outcomes suggested an increase in the maximum temperature for all months. The magnitude of the increase peaked in the summer, with a small change in the winter. Considering the average of all the five models, the average increase was maximum in August (0.87 °C in the 2020s, 1.75 °C in the 2050s and 2.40 °C in the 2080s) and minimum in February (0.37 °C in the 2020s) and March (1.14 °C in the 2050s and 1.60 °C in the 2080s). All the models predicted an increase in temperature in future time slices, with the maximum increase in the 2080s and the minimum in the 2020s. The average yearly change considering all five models was 0.68 °C in the 2020s, 1.5 °C in the 2050s, and 2.03 °C in the 2080s.

Under the RCP 8.5 scenario, the average maximum temperature was projected to increase by all the models in all the months except March, where the maximum temperature decreased for ACCESS 1.0 and NorESM1-M under the RCP 8.5 scenario for the 2020s. Average maximum temperature was observed maximum in April in the 2020s and 2050s (17.95 °C in the 2020s and 19.06 °C in the 2050s), in July (20.78 °C) in the 2080s, and minimum in December–January (9.32 °C in the 2020s, 10.78 °C in the 2050s, and 12.38 °C in the 2080s) following almost the same trend as the baseline period (Table 1). The average maximum temperature was projected to increase by all the models in all the months in

**Table 3** Monthly changes in total precipitation (mm) under different RCP scenarios

Mon	RCP 8.5																	
	RCP 4.5			2050s			2080s			2020			2050			2080		
	Avg value	Change %	Avg value	Change %	Avg value	Change %	Avg value	Change %	Avg value	Change %	Avg value	Change %	Avg value	Change %	Avg value	Change %		
Jan	1.71	36.81	2.34	10.99	1.90	4.72	1.79	4.72	2.25	31.20	1.84	7.51	11.80	1.17	11.80	1.17		
Feb	2.87	7.62	3.09	11.57	3.20	5.43	3.02	5.43	3.27	14.17	4.01	39.93	39.87	1.93	39.87	1.93		
Mar	7.11	19.91	8.52	12.07	7.97	13.08	8.04	13.08	8.17	15.00	8.74	22.97	29.97	2.01	29.97	2.01		
Apr	15.32	0.11	15.34	-0.63	15.22	-3.76	14.74	-3.76	14.43	-5.82	15.35	0.18	4.09	3.26	4.09	3.26		
May	24.91	-4.01	23.91	-0.82	24.70	3.53	25.79	3.53	27.12	8.89	25.25	1.36	-3.21	7.66	-3.21	7.66		
Jun	28.31	6.84	30.25	-3.48	27.33	-3.92	27.20	-3.92	28.43	0.40	27.07	-4.39	-6.09	4.68	-6.09	4.68		
Jul	19.08	-7.40	17.66	0.48	19.17	-8.75	17.41	-8.75	19.49	2.16	16.19	-15.14	-11.73	4.45	-11.73	4.45		
Aug	17.89	2.16	18.27	-10.73	15.97	-21.22	14.09	-21.22	17.05	-4.67	15.30	-14.48	-21.62	3.43	-21.62	3.43		
Sep	17.31	1.60	17.59	2.47	17.74	-2.66	16.85	-2.66	16.70	-3.54	16.77	-3.15	-7.26	5.88	-7.26	5.88		
Oct	8.71	-8.26	7.99	-3.48	8.41	-5.75	8.21	-5.75	8.25	-5.37	8.59	-1.37	9.06	2.10	9.06	2.10		
Nov	2.44	9.78	2.68	11.10	2.71	10.06	2.69	10.06	3.00	22.71	3.04	24.41	15.19	1.15	15.19	1.15		
Dec	1.39	52.39	2.12	1.44	1.41	1.76	1.42	1.76	1.94	39.45	1.58	13.88	15.80	0.66	15.80	0.66		

all three future time slices, with the maximum increase in the 2080s and the minimum increase in the 2020s. Considering the average of all the five models, the average increase in maximum temperature was maximum in April in the 2020s (1.03 °C) and in August in the 2050s (2.48 °C) and 2080s (4.53 °C), and minimum in March (0.61 °C in the 2020s, 1.60 °C in the 2050s and 3.05 °C in the 2080s). The average yearly change considering all the five models was 0.90 °C in the 2020s, 2.19 °C in the 2050s, and 3.88 °C in the 2080s). Changes in maximum temperature ranged from 0.37 to 4.53 °C for the present study, which goes well with the findings of Bhandari et al. (2020), where they estimated that maximum temperature changes fluctuate between 1.6 °C to 4.01 °C for Pajaro River Watershed (PRW) of central California.

**Minimum temperature envelope under projected climatic scenarios**

The average projected minimum temperature was observed at its minimum in January, then gradually increased up to July, and again decreased up to December in the baseline period as well as in future time slices (Fig. 6 and Table 2).

Under the RCP 4.5 scenario, average minimum temperature was observed at its maximum in the month of July in all the future time slices (11.14 °C in the 2020s, 12.35 °C in the 2050s, and 12.91 °C in the 2080s) and minimum in January (- 2.54 °C in the 2020s and - 2.00 °C in the 2050s) and December (- 1.59 °C in the 2080s) (Table 2). Minimum temperature was observed maximum in 2080s and minimum in 2020s. The average minimum temperature increased in all the months in all three future time slices. On monthly basis, considering all the five models, the average increase was maximum in July (0.73 °C in the 2020s and 2.23 °C in the 2080s) and in November in the 2050s (1.70 °C). Average increase was minimum in February (0.26 °C in 2020s) and January in 2050s (0.89 °C) and 2080s (1.32 °C). The range of projections varied from 0.08 °C to 1.87 °C. The average yearly change considering all five models was 0.55 °C, 1.3 °C, and 1.82 °C in the 2020s, 2050s, and 2080s, respectively.

Under the RCP 8.5 scenario, the average minimum temperature was observed to be at its maximum in the month of July in all the future time slices (11.48 °C in the 2020s, 13.06 °C in the 2050s, 14.74 °C in the 2080s) and at its minimum in December (- 2.60 °C in the 2020s and - 1.31 °C in the 2050s) and January (0.24 °C in the 2080s) (Table 2). The minimum temperature was observed at its maximum in the 2080s and minimum in the 2020s. The average minimum temperature increased in all the months in all three future time slices. On monthly basis, considering all five models, the average increase was maximum in April (0.83 °C in the 2020s) and in October in the 2050s (2.57 °C) and 2080s

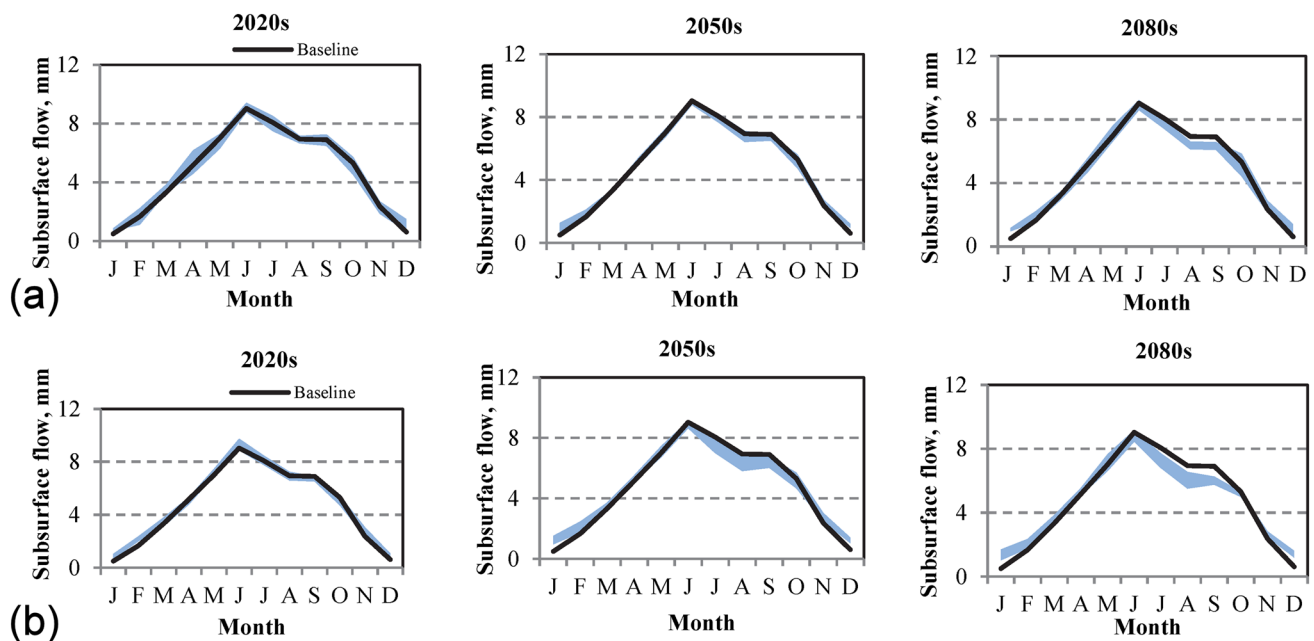


**Fig. 8** RHESSys simulated subsurface flow ranges under: **a** RCP 4.5 scenario, **b** RCP 8.5 scenario

(4.21 °C). The average increase was minimum in December (0.38 °C in the 2020s), January in 2050s (1.65 °C), and April in the 2080s (2.90 °C). The range of projection varied from 0.20 °C to 1.27 °C. The average yearly change considering all five models was 0.71 °C, 2.04 °C, and 3.61 °C in the 2020s, 2050s, and 2080s, respectively. The increase in average minimum temperature was high in the high emission scenario (RCP 8.5) as compared to RCP 4.5 in all three future time slices.

For the 2020s, the magnitudes of temperature increase (both maximum and minimum temperature) for RCP4.5 and RCP8.5 are almost alike (with an increase value below 1 °C in all the months), as the difference between the two RCPs before 2050 are minor. After 2050, both scenarios show very different features, and the temperature increase for RCP 8.5 reaches around 4–5° under RCP 8.5, whereas the temperature increases by around 1–2° under the RCP 4.5 scenario by 2100. Changes in minimum temperature ranged from 0.38 to 4.21 °C for the present study, which matches well with the findings of Maharjan et al. (2021), where they estimated that minimum temperature changes fluctuate between 0.7 °C to 4.9 °C for the Thuli Bheri River Basin, Nepal.

### Precipitation envelope under projected climatic scenarios

Total projected precipitation was observed at its minimum in January, then increased gradually up to June, and again decreased up to December in the baseline period as well as

in future time slices (Fig. 7 and Table 3). The future projection of total precipitation shows certain similarities across both scenarios, with an increase in precipitation in the winter months and a decrease in the monsoon months as compared to the baseline period. These changes are most pronounced in the high emissions (RCP8.5) scenario as compared to the RCP 4.5 scenario.

Under the RCP 4.5 scenario, total precipitation was observed to be maximum in June (30.25 mm in the 2020s, 27.33 mm in the 2050s, and 27.20 mm in the 2080s) and minimum in December (2.12 mm in the 2020s, 1.41 mm in the 2050s, and 1.42 mm in the 2080s) in all three future time slices (Table 3). Total precipitation increased in winter months and decreased in monsoon months in all time slices. The maximum increase was observed in the month of December in 2020s (52.39%) and in March in 2050s (12.07%) and 2080s (13.08%). The maximum decrease was in October (− 8.26%) in the 2020s and in August in the 2050s (− 10.73%) and 2080s (− 21.22%). On a yearly basis, considering the average of all the five models, precipitation was observed to increase by around 1.85% in the 2020s and decrease by around 0.90% and 3.94% in the 2050s and 2080s, respectively, as compared to the baseline period.

Under the RCP 8.5 scenario also, total precipitation was observed at its maximum in June (28.43 mm in the 2020s, 27.07 mm in the 2050s, and 26.59 mm in the 2080s) and at its minimum in December (1.94 mm in the 2020s, 1.58 mm in the 2050s, and 1.61 mm in the 2080s) in all three future time slices (Table 3). According to the outcome, monsoon

**Table 4** Monthly changes in average subsurface flow (mm) under different RCP scenarios

Mon	RCP 8.5																	
	RCP 4.5			2050s			2080s			2020			2050			2080		
	Avg value	Change %	Avg value	Change %	Avg value	Change %	Avg value	Change %	Avg value	Change %	Avg value	Change %	Avg value	Change %	Avg value	Change %		
Jan	0.50	56.98	0.79	0.94	87.67	115.29	0.21	0.87	73.49	136.42	0.55	182.23	0.67					
Feb	1.66	11.54	1.85	1.89	13.68	1.17	0.71	2.13	28.12	30.68	0.74	24.93	0.60					
Mar	3.33	5.67	3.52	3.33	0.09	-6.14	0.55	3.48	4.38	4.85	0.55	7.91	0.53					
Apr	5.16	1.73	5.25	5.20	0.75	-5.74	0.90	5.11	-0.99	2.75	0.44	5.12	0.47					
May	7.01	-2.23	6.85	6.98	-0.46	-0.47	1.01	7.18	2.39	1.98	0.74	0.24	1.05					
Jun	9.04	1.48	9.17	8.90	-1.49	-3.72	0.64	9.26	2.42	-1.91	0.49	-3.21	0.74					
Jul	8.06	-0.89	7.98	7.96	-1.24	-1.42	0.56	8.10	0.58	-7.67	1.08	-6.77	0.92					
Aug	6.93	-0.61	6.89	6.69	-3.51	-8.38	0.50	6.95	0.28	-7.84	1.19	-11.57	1.04					
Sep	6.90	-0.57	6.86	6.70	-2.83	-11.65	0.48	6.71	-2.73	-7.30	0.72	-10.97	0.51					
Oct	5.31	-5.24	5.03	5.20	-2.00	-16.98	1.44	5.09	-4.15	-2.84	1.04	0.12	0.33					
Nov	2.36	4.12	2.46	2.58	9.13	-8.97	0.76	2.65	12.37	14.97	0.57	14.77	0.37					
Dec	0.61	54.52	0.95	1.05	70.96	58.01	0.57	0.88	43.31	106.09	0.36	131.91	0.42					

months would exhibit a deficit in rainfall amount, whereas winter months would receive more rainfall as compared to the baseline period. The maximum increase was observed in the months of December in the 2020s (39.45%) and February in the 2050s (39.33%) and 2080s (39.87%). Maximum decreases were in April (- 5.82%) in the 2020s, in July in the 2050s (- 15.14%) and in August in the 2080s (- 21.62%). The range of projection varied from 0.66 to 7.66 mm. On a yearly basis, model-average total precipitation increased in the 2020s (2.07% increase) and decreased in the 2050s (2.26% decrease) and 2080s (2.99% decrease) as compared to the baseline period.

Both the RCP scenarios show an increase in annual precipitation in the near future (2020s), and it is expected to decrease in the 2050s and the 2080. The projections show a prevalent summertime drying (with precipitation up to 20% lower than present-day average values), while the winter experiences higher precipitation (up to 50% higher than at present). The relative change in seasonal precipitation (especially for drier months) is significantly larger than the annual mean change. These changes in rainfall amount are expected to affect yearly and monthly streamflow at the catchment outlet. Percentage changes in monthly precipitation ranged from -21% to 52.39% for the watershed, which agrees well with the findings of Maharjan et al. (2021), where they estimated that precipitation changes fluctuate between - 12 and 50% for Thuli Bheri River Basin, Nepal.

**Change in hydrological variables with climate change**

Future climate data (maximum and minimum temperature and precipitation) from different CMIP5 models were used as climate inputs in the already calibrated and validated RHESSys model to simulate future subsurface flow, overland flow, total streamflow, and saturation deficit. RHESSys uses TOPMODEL (Beven and Kirkby 1979) for the simulation of saturation deficit and streamflow. Daily values were averaged to obtain monthly values for better analysis.

**Subsurface flow**

The total subsurface flow was at its minimum in January, increased gradually to reach its maximum in June, and again reduced gradually up to December for both the baseline period and all future simulations. The pattern of subsurface flow fluctuation followed the same trend as total precipitation (Fig. 8 and Table 4).

Under the RCP 4.5 scenario, taking the average of all the five models, the maximum subsurface flow was observed in June (9.17 mm in the 2020s, 8.90 mm in the 2050s, and 8.87 mm in the 2080s) and the minimum in January



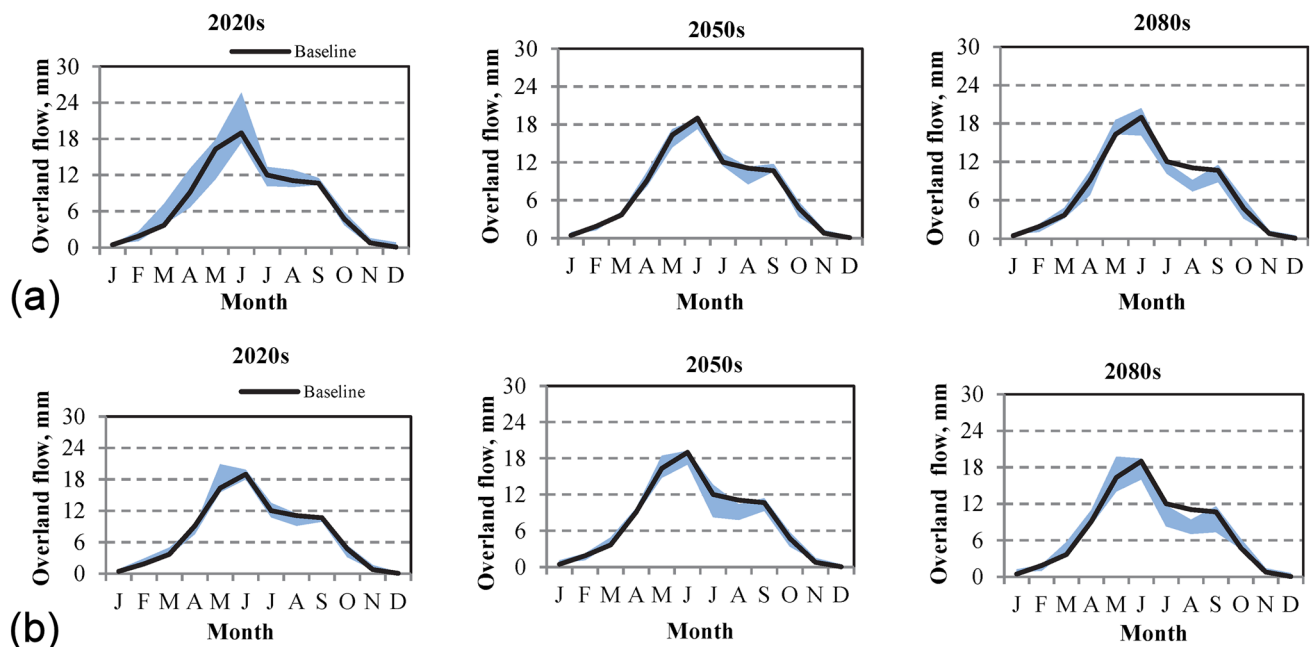


**Fig. 9** RHESSys simulated overland flow ranges under: **a** RCP 4.5 scenario, **b** RCP 8.5 scenario

(0.79 mm in the 2020s, 0.94 mm in the 2050s, and 1.09 mm in the 2080s) in all three future time slices (Table 4). On a monthly basis, total subsurface flow increased in the winter and decreased in the summer months, following the same trend as total precipitation. Taking the average of all the five models, the percentage increase in subsurface flow was maximum in January (56.98% for the 2020s, 87.67% for the 2050s, and 111.25% for the 2080s), and the percentage decrease was maximum in October (− 5.24% for the 2020s and − 16.98% for the 2080s) and in August (− 3.51%) in the 2050s. The range of projection varied from 0.13 to 1.60 mm. Model-average total subsurface flow increased in the 2020s (1.29% increase) and 2050s (0.96% decrease) and decreased in the 2080s (1.09% decrease) as compared to the baseline period.

Under the RCP 8.5 scenario, taking the average of all the five models, the maximum subsurface flow was observed in June (9.26 mm in the 2020s, 8.86 mm in the 2050s, and 8.75 mm in the 2080s) and the minimum in January (0.87 mm in the 2020s, 1.18 mm in the 2050s, and 1.41 mm in the 2080s) in all three future time slices (Table 4). On a monthly basis, total subsurface flow increased in the wintertime and decreased in the summertime, following the same trend as precipitation. Taking the average of all the five models, the percentage increase was maximum in January (73.49% in the 2020s, 136.42% in the 2050s, and 182.23% in the 2080s) and the percentage decrease was maximum in October (− 4.15%) in the 2020s and in August in the 2050s (− 7.84%) and 2080s (− 11.57%). Considering the yearly average, total subsurface flow in 2020s increased for

all the models except MPI-ESM-LR (− 0.17% decrease), the maximum increase in subsurface flow was for ACCESS 1.0 (4.11%), whereas in 2050s it increased for all the models except CCSM 4 and CNRM-CM5, the maximum increase was for MPI-ESM-LR (6.11%); and the maximum decrease was for CNRM-CM5 (3.8% decrease). In the 2080s, total subsurface flow increased for all the models except CNRM-CM5 (0.78% decrease), the maximum increase was for ACCESS 1.0 (4.11% increase). Model-average total subsurface flow increased in all three future time slices in 2020s (2.69%, 1.14% and, 1.12% increase in 2020s, 2050s, and 2080s, respectively as compared to the baseline period). On the yearly basis, under both RCPs, the percentage change in the model-average subsurface flow reduced gradually from 2020 to 2080, whereas under RCP 4.5, it was found to be decreasing in 2080s.

### Overland flow

The total overland flow was minimum in December–January and maximum in June for both the baseline period as well as all future simulations. The pattern of overland flow fluctuation followed the same trend as total precipitation (Fig. 9 and Table 5). The range of projections from five models for each time slice was observed to be high in summer months and low in winter months.

Under the RCP 4.5 scenario, taking the average of all the five models, the maximum overland flow was observed in June (20.53 mm in the 2020s, 18.29 mm in the 2050s, and 18.20 mm in the 2080s) and the minimum in December

**Table 5** Monthly changes in average overland flow (mm) under different RCP scenarios

Mon	RCP 8.5												
	RCP 4.5			2020s			2050s			2080s			
	Baseline	Avg value	Change %	Avg value	Change %	Avg value	Change %	Avg value	Change %	Avg value	Change %	Avg value	Change %
Jan	0.45	0.59	32.72	0.68	53.26	0.75	62.82	0.67	50.06	0.82	83.59	0.97	118.29
Feb	1.86	1.98	6.52	1.60	-14.16	1.42	-41.13	2.26	21.13	1.82	-2.41	1.58	-15.31
Mar	3.68	4.88	32.80	3.94	7.30	3.98	7.19	4.19	13.99	4.42	20.28	4.80	30.55
Apr	9.09	9.28	2.04	9.08	-0.15	8.75	-14.65	8.53	-6.22	9.18	0.92	9.59	5.46
May	16.32	15.59	-4.47	16.17	-0.91	17.00	3.10	18.00	10.26	16.62	1.79	15.78	-3.34
Jun	19.01	20.53	8.04	18.29	-3.74	18.20	-7.27	19.13	0.64	18.09	-4.82	17.73	-6.74
Jul	12.02	11.07	-7.91	12.13	0.91	10.77	-1.04	12.32	2.50	9.94	-17.32	10.45	-13.07
Aug	11.06	11.38	2.82	9.65	-12.81	8.32	-23.68	10.49	-5.19	9.16	-17.22	8.22	-25.72
Sep	10.66	10.95	2.63	11.01	3.20	10.29	-17.13	10.25	-3.86	10.25	-3.91	9.75	-8.55
Oct	4.74	4.35	-8.16	4.47	-5.61	4.39	-33.75	4.30	-9.19	4.61	-2.78	5.21	10.01
Nov	0.77	1.00	29.38	1.04	34.55	1.00	5.21	1.19	54.83	1.20	56.18	1.11	44.14
Dec	0.07	0.29	288.36	0.24	225.17	0.29	217.14	0.19	152.60	0.35	367.98	0.48	546.16

(0.29 mm in the 2020s and 2080s and 0.24 mm in the 2050s) in all three future time slices (Table 5). The monthly projections show significant decreases in overland flow in summertime, while significant increases in wintertime are indicated following a similar trend of precipitation. On a monthly basis, taking the average of all the five models, the percentage increase in overland flow was maximum in December (288.36% in the 2020s, 225.17% in the 2050s, and 217.14% in the 2080s) in all three future time slices. The percentage decrease was maximum in October (- 8.16%), August (- 12.81%), and February (- 41.13%) in the 2020s, 2050s, and 2080s, respectively.

Under the RCP 8.5 scenario, taking the average of all the five models, the maximum overland flow was observed in June (19.13 mm in the 2020s, 18.09 mm in the 2050s, and 17.73 mm in the 2080s) and minimum in December (0.19 mm in the 2020s, 0.35 mm in the 2050s, and 0.48 mm in the 2080s) in all three future time slices (Table 5). The monthly projections show significant decreases of overland flow in summertime, while significant increases in wintertime are indicated in all three future time slices following the similar trend of precipitation; however, changes are maximum in the 2080s and minimum in the 2020s. On monthly basis, taking the average of all the five models, the percentage increase was maximum in December (152.60% in the 2020s, 367.98% in the 2050s, and 546.16% in the 2080s), and the percentage decrease was maximum in October (- 9.19%) in the 2020s, and in July (- 17.32%) and August (- 25.72%) in the 2050s and 2080s, respectively. The range of projection varied from 0.20 mm to 5.73 mm. Considering the yearly average, model-average total overland flow increased in the 2020s (1.98% increase) and decreased in the 2050s (3.67% decrease) and 2080s (4.54% decrease) as compared to the baseline period. Considering yearly average, model-average total overland flow increased in 2020s (2.40% increase) and decreased in 2050s (- 1.60%) and 2080s (- 5.10%) as compared to the baseline period, following the same trend as the yearly change in total precipitation.

**Total streamflow**

Total streamflow gradually increased from January to June, after which it reduced gradually to December. Streamflow was as its maximum during May-June-July, and the minimum values were in December-January. This overall pattern and the change in streamflow varied directly with the precipitation pattern. Figure 10 and Table 6 show the future change rates of monthly total streamflow for different projected scenarios of climate change.

Under the RCP 4.5 scenario, in the 2020s, taking the average of all the five models, maximum streamflow was observed in June (29.70 mm in the 2020s, 27.20 mm in the 2050s, and 27.08 mm in the 2080s) and minimum in

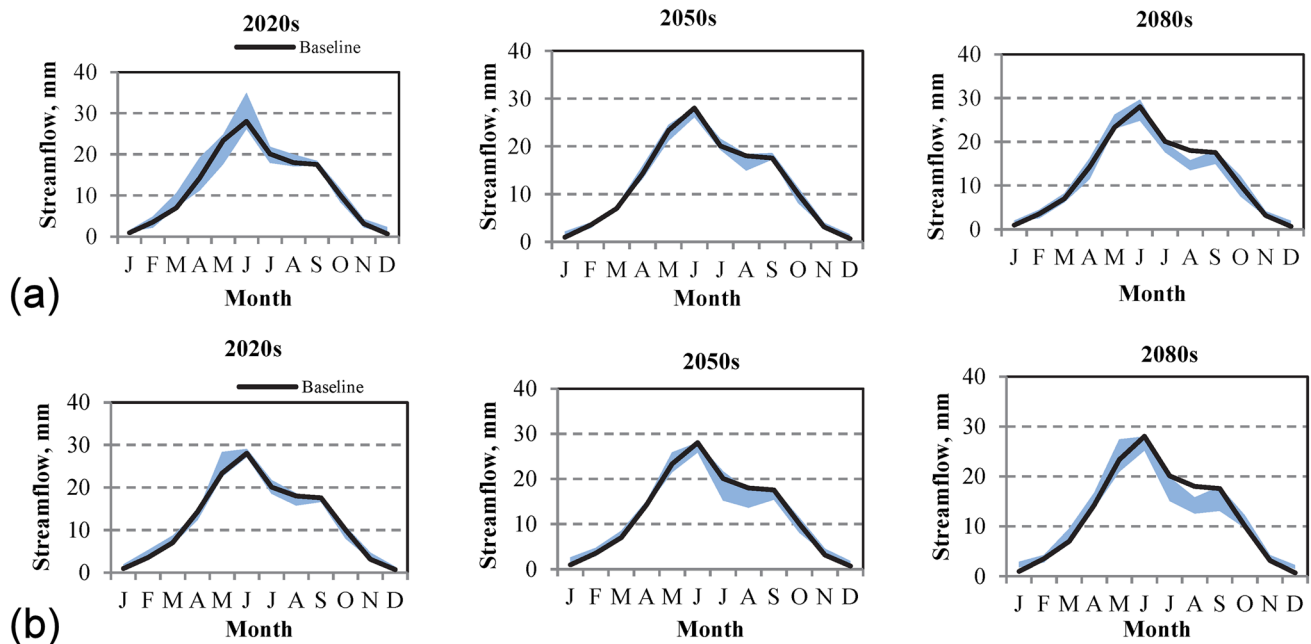


**Fig. 10** RHESSys simulated streamflow ranges under: **a** RCP 4.5 scenario, **b** RCP 8.5 scenario

December (1.23 mm in the 2020s, 1.29 mm in the 2050s, and 1.38 mm in the 2080s) (Table 6). At the monthly scale, it was found that total streamflow increased significantly in wintertime (November to March) and decreased in summertime for all projected time slices, following the same trend as the change in monthly precipitation. The average percentage increase in total streamflow was maximum in December (79.68% in the 2020s, 87.55% in the 2050s and, 100.74% in the 2080s), and the average percentage decrease was maximum in October (− 6.62% in the 2020s) and August (− 9.23% in the 2050s and − 18.68% in the 2080s). At the annual scale, the RCP 4.5 scenario predicts about a 1.97% increase in total streamflow in the 2020s and a deficit of about 0.60% and 3.54% in the 2050s and 2080s, respectively, as compared to the baseline period.

Under the RCP 8.5 scenario, in the 2020s, taking the average of all the five models, maximum streamflow was observed in June (28.38 mm in the 2020s, 26.95 mm in the 2050s, and 26.47 mm in the 2080s) and minimum in December (1.06 mm in the 2020s, 1.61 mm in the 2050s, and 1.90 mm in the 2080s) (Table 6). At the monthly scale, it was found that total streamflow increased significantly in wintertime (November to March) and decreased in summertime for all projected time slices, following the same trend as the change in monthly precipitation. The average percentage increase was maximum in January (62.44% in 2020s) and in December in the 2050s (134.27%) and 2080s (176.48%), and the average percentage decrease was maximum in October (− 6.52% in 2020s) and in August in the 2050s (− 13.60%) and 2080s (− 20.21). At the annual scale, the model-average

predicted streamflow increased by 2.26% in the 2020s and reduced by around 1.81% and 2.34% in the 2050s and 2080s, respectively (Table 6), as compared to the baseline period.

Monthly and annual total streamflow at the watershed outlet is greatly affected by changes in precipitation amounts over the three projected time slices and for both RCP4.5 and RCP8.5. The increase in flows in the 2020s can be explained by the increase in rainfall over the watershed during this period under both RCPs, whereas the flow deficit in the 2050s and 2080s can be explained by the decrease in precipitation during those periods under both RCPs.

### Saturation deficit

Total saturation deficit was observed high in January, then decreased gradually and remained low during April–September with a slight increase in the middle around May–June, after which it increased gradually again to reach the maximum in December, following the reverse trend of precipitation. This overall pattern was found to be the same in both the baseline period as well as all future simulations (Fig. 11 and Table 7).

Under the RCP 4.5 scenario, taking the average of all the five models, the maximum saturation deficit was observed in December (614.38 mm in the 2020s, 604.34 mm in the 2050s, and 595.26 mm in the 2080s) in all three future time slices, and the minimum in August (246.78 mm in the 2020s) and September (237.65 mm in the 2050s and 235.97 mm in the 2080s) (Table 7). The monthly projections show significant increases in saturation deficit in

**Table 6** Monthly changes in average streamflow (mm) under different RCP scenarios

Mon	Baseline	RCP 4.5						RCP 8.5					
		2020s		2050s		2080s		2020		2050		2080	
		Avg value	Change %	Avg value	Change %	Avg value	Change %	Avg value	Change %	Avg value	Change %	Avg value	Change %
Jan	0.95	1.38	45.54	1.62	71.44	1.85	1.54	62.44	2.00	111.50	2.39	152.07	
Feb	3.52	3.84	8.89	3.49	-1.03	3.24	4.39	24.43	3.99	13.20	3.65	3.67	
Mar	7.01	8.40	19.91	7.28	3.87	7.22	7.67	9.42	7.91	12.95	8.39	19.79	
Apr	14.26	14.53	1.93	14.28	0.18	13.87	13.64	-4.33	14.48	1.58	15.02	5.34	
May	23.33	22.45	-3.79	23.15	-0.78	24.15	25.17	7.90	23.76	1.85	22.80	-2.27	
Jun	28.04	29.70	5.92	27.20	-3.02	27.08	28.38	1.21	26.95	-3.88	26.47	-5.60	
Jul	20.08	19.06	-5.09	20.09	0.04	18.43	20.43	1.73	17.38	-13.45	17.96	-10.55	
Aug	17.99	18.26	1.50	16.33	-9.23	14.63	17.44	-3.08	15.55	-13.60	14.35	-20.27	
Sep	17.56	17.80	1.37	17.71	0.83	16.59	16.96	-3.42	16.64	-5.24	15.89	-9.50	
Oct	10.05	9.38	-6.62	9.68	-3.70	9.46	9.39	-6.52	9.76	-2.81	10.53	4.78	
Nov	3.13	3.46	10.34	3.61	15.39	3.52	3.85	22.82	3.92	25.11	3.82	21.99	
Dec	0.69	1.23	79.68	1.29	87.55	1.38	1.06	55.07	1.61	134.27	1.90	176.48	

summertime, while significant decreases in wintertime are indicated, which follows the inverse trend of the change in total precipitation. On the monthly basis, taking the average of all the five models, the percentage increase in saturation deficit was maximum in April (10.69%), June (5.81%), and May (6.73%) in the 2020s, 2050s, and 2080s, respectively, and the percentage decrease was maximum in December (-5.37% in the 2020s) and January (-7.26% in the 2050s and -9.01% in the 2080s). Considering the annual average, the model-average predicted saturation deficit increased by 0.85% in the 2020s and reduced by around 2.36% and 1.63% in the 2050s and 2080s, respectively, as compared to the baseline period.

Under the RCP 8.5 scenario, taking the average of all the five models, the maximum saturation deficit was observed in December (624.40 mm in the 2020s, 581.98 mm in the 2050s, and 557.40 mm in the 2080s) in all three future time slices, and the minimum in August (237.03 mm in the 2020s) and April (241.59 mm in the 2050s and 238.58 mm in the 2080s) (Table 7). The monthly projections show significant increases in saturation deficit in summertime, while significant decreases in wintertime are indicated, which follows the inverse trend of the change in total precipitation. On the monthly basis, taking the average of all the five models, the percentage increase in saturation deficit was maximum in April (5.62%), May (5.05%), and August (10.22%) in the 2020s, 2050s, and 2080s, respectively, and the percentage decrease was maximum in January (-6.58% in the 2020s, -11.37% in the 2050s and -14.74% in the 2080s). The range of projection varied from 8.97 to 79.16 mm. Considering annual variation, the model-average saturation deficit decreased in all future time slices as compared to the baseline period, with a minimum decrease in the 2020s (-2.34%), then in the 2050s (-4.14%), and the 2080s (-5.12%).

### Sensitivity of hydrological variables to climate change

The sensitivity of variables to climate change was analyzed for all future time slices (2020s, 2050s, and 2080s) and for both the RCP scenarios separately. Average percentage changes in each variable were analyzed, and the variables were ranked in order of their sensitivity to climate change (Table 8). Variables like streamflow and overland flow are directly dependent on rainfall; thus, they vary directly with variation in rainfall in all the future time slices, whereas saturation deficit depends on temperature, precipitation, and other variables like PET, which in a way depends on temperature, RH, and other variables.

In the 2020s, under the RCP 4.5 scenario, overland flow was found to be most sensitive to climate change, with a 2.4% increase as compared to the baseline period,

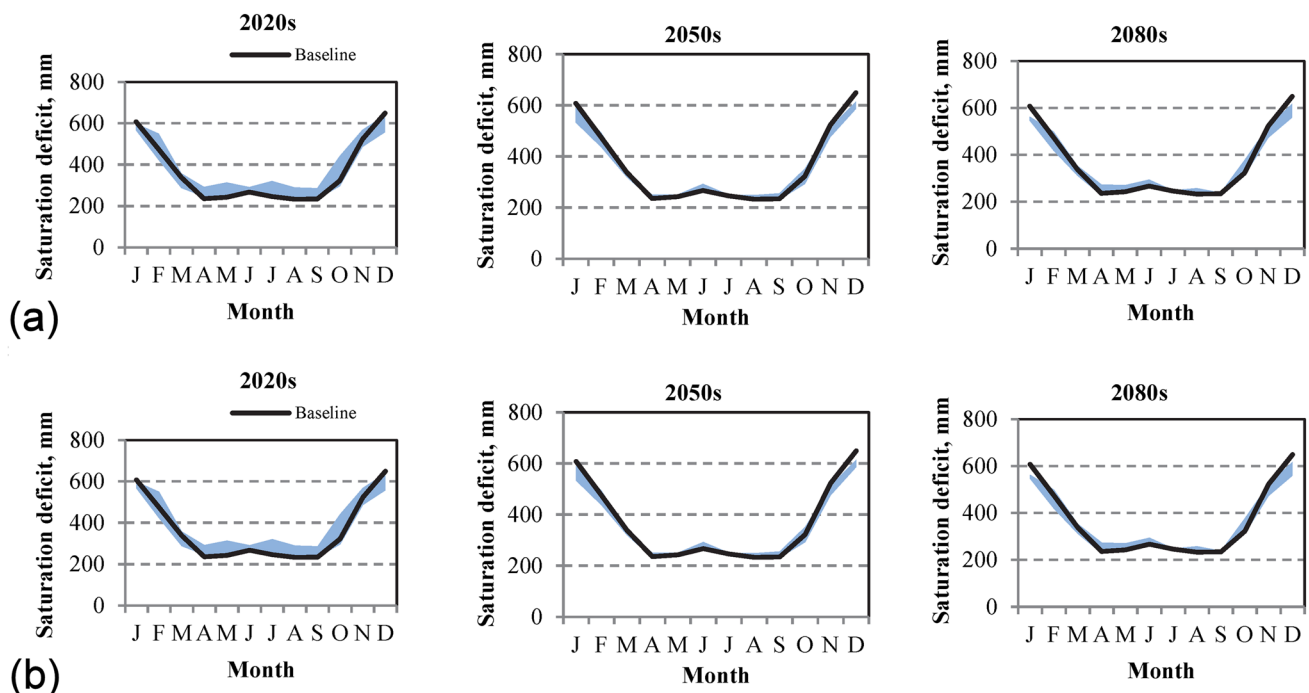


**Fig. 11** RHESSys simulated saturation deficit ranges under: **a** RCP 4.5 scenario, **b** RCP 8.5 scenario

followed by streamflow (1.97% increase) and subsurface flow (1.29% increase). In the 2050s, the subsurface flow was observed decreasing while other variables increased. The saturation deficit was found to be most sensitive to climate change, with a 2.36% decrease, followed by overland flow (1.60% decrease) and subsurface flow (0.96% increase). All the variables were observed to decrease in the 2080s under the RCP 4.5 scenario. The overland flow was found to be most sensitive to climate change, with a 5.09% decrease from the baseline period, followed by streamflow (3.54% decrease) and saturation deficit (1.62% decrease).

Under RCP 8.5 in the 2020s, the subsurface flow was found to be most sensitive to climate change, with a 2.69% increase as compared to the baseline period, followed by saturation deficit (2.34% decrease) and streamflow (226% increase). In the 2050s, saturation deficit was found to be most sensitive to climate change with a 4.44% decrease as compared to the baseline period, followed by overland flow (3.67% decrease) and streamflow (1.81% decrease), and in the 2080s, saturation deficit was found to be most sensitive to climate change with a 5.11% decrease as compared to the baseline period, followed by overland flow (3.66% decrease) and streamflow (2.34% decrease).

### Comparison of projected streamflow with observed streamflow

Streamflow generated for the depletion period (April–September) of 2016 from RHESSys simulations using climate forcing projected under RCP 4.5 and RCP 8.5 scenarios was compared with the observed streamflow. Total runoff for the RCP 4.5 scenario varied from 183.85 to 214.20  $M m^3$  with an average of 197.44  $M m^3$ , whereas under the RCP 8.5 scenario, total runoff varied from 140.04 to 236.38  $M m^3$  with an average of 202.718  $M m^3$ . The actual streamflow for the year 2016 was obtained using the observed stage data at the watershed outlet. Observed daily stage data were converted to corresponding discharge using the developed stage discharge curve. Total observed discharge in the depletion period of 2016 was obtained as 199.02  $M m^3$ . The total simulated discharge obtained for the same period for all the CMIP5 models under both the RCP scenarios was quite comparable with the observed value. Under the RCP 4.5 scenario, the deviation of simulated streamflow from the observed varied from 15.18 to  $-15.17 M m^3$ , and the average runoff simulated for different models was quite comparable (around 1.58  $M m^3$  less than the observed) with the observed value. Under the RCP 8.5 scenario, the deviation of simulated streamflow from the observed varied from 37.36



**Table 7** Monthly changes in average saturation deficit (mm) under different RCP scenarios

Mon	Baseline	RCP 4.5						RCP 8.5					
		2020s		2050s		2080s		2020		2050		2080	
		Avg value	Change %	Avg value	Change %	Avg value	Change %	Avg value	Change %	Avg value	Change %	Avg value	Change %
Jan	607.46	- 4.49	563.38	- 7.26	552.72	- 9.01	567.47	- 6.58	538.40	- 11.37	517.94	- 14.74	
Feb	474.22	- 2.28	458.94	- 3.22	470.56	- 0.77	435.90	- 8.08	432.24	- 8.85	446.87	- 5.77	
Mar	337.98	- 3.72	327.83	- 3.00	335.06	- 0.86	327.17	- 3.20	316.31	- 6.41	307.38	- 9.05	
Apr	235.79	10.69	241.14	2.27	248.75	5.49	249.05	5.62	241.59	2.46	238.58	1.18	
May	242.35	8.65	246.01	1.51	258.64	6.73	253.83	4.74	254.58	5.05	255.12	5.27	
Jun	267.01	5.98	282.51	5.81	279.21	4.57	275.80	3.29	276.54	3.57	270.56	1.33	
Jul	245.62	6.05	245.95	0.13	242.73	- 1.18	245.71	0.04	254.18	3.48	250.52	1.99	
Aug	233.16	5.84	242.46	3.98	246.42	5.68	237.03	1.66	243.21	4.31	256.98	10.22	
Sep	234.08	7.46	237.65	1.52	235.97	0.81	241.61	3.22	239.98	2.52	247.36	5.67	
Oct	322.26	8.30	322.40	0.04	337.74	4.80	321.95	- 0.10	318.63	- 1.13	310.74	- 3.57	
Nov	522.68	- 2.37	495.93	- 5.12	497.72	- 4.78	489.49	- 6.35	480.15	- 8.14	488.62	- 6.52	
Dec	649.27	- 5.37	604.34	- 6.92	595.26	- 8.32	624.40	- 3.83	581.98	- 10.36	557.40	- 14.15	

to 58.99 M m<sup>3</sup>, and the average runoff simulated for different models was around 3.69 M m<sup>3</sup> more than the observed. Overall, the streamflow estimated under the RCP 4.5 scenario was more comparable with the observed streamflow, with an average deviation of - 1.58 M m<sup>3</sup> (Table 9).

### Conclusions

Hydrological models are increasingly used for the assessment of the sensitivity of hydrologic variables to climate change. In the present study, an effort has been made to investigate the potential hydrologic responses to projected climatic scenarios by applying the RHESSys model. In this study, the analysis of the hydrologic response of the Nuranang watershed to the changed climate was mainly focused on predicting the potential effects of changes in temperature and precipitation on total streamflow and saturation deficit. Daily maximum and minimum temperatures and precipitation for the present climate (1979–2005) and future years (2006–2097) from CORDEX were used as climate forcing in the RHESSys model. The model was first calibrated and validated for the watershed; the calibrated model was further used to investigate the climate change impact on streamflow and saturation deficit. All the GCMs indicated that the study region would be warmer in the twenty-first century, with average temperature increasing between 1.39 and 6.39 °C as compared to the baseline period. The model-average total precipitation increased in the 2020s but decreased in the 2050s and 2080s under both RCP scenarios. Monthly, the projections show around a 20% decrease in precipitation during the summer while the winter experiences higher precipitation (up to 50% higher than at present). These seasonal changes in precipitation amount greatly affect yearly and monthly streamflow at the watershed outlet. Variations in subsurface flow, overland flow, and streamflow in future time slices followed almost the same trend as changes in precipitation. Temperature increases during summer increase evaporation and reduce flows, whereas temperature increases during winter produce greater snowmelt rates when a snowpack is present or cause precipitation to occur as rain instead of snow. Greater snowmelt rates and rain rather than snowfall both cause a small increase in streamflow in the winter season. On a monthly scale, subsurface flow, overland flow, and total streamflow increased significantly in wintertime and decreased in summertime compared to the baseline period, following the same trend as precipitation. Total saturation deficit was observed to be high in January, then decreased gradually and remained low during April–September with a slight increase in the middle around May–June, after which it increased gradually again to reach a maximum in December, following a reverse trend of precipitation. Overland flow and total streamflow were

**Table 8** Change in hydrological variables under different RCP scenarios

Hydrological Variable	RCP 4.5						RCP 8.5					
	2020		2050		2080		2020		2050		2080	
	Change %	Rank	Change %	Rank	Change %	Rank	Change %	Rank	Change %	Rank	Change %	Rank
Subsurface flow	1.29	3	0.96	3	-1.08	4	2.69	1	1.14	4	1.12	4
Overland flow	2.40	1	-1.60	2	-5.09	1	-1.98	4	-3.67	2	-3.66	2
Total Streamflow	1.97	2	-0.60	4	-3.54	2	2.26	3	-1.81	3	-2.34	3
Saturation deficit	0.85	4	-2.36	1	-1.62	3	-2.34	2	-4.44	1	-5.11	1

**Table 9** Total simulated streamflow under RCP 4.5 and RCP 8.5 scenarios with different climate model projections

Model	Simulation period	Total observed streamflow, M m <sup>3</sup>	RCP 4.5		RCP 8.5	
			Total RHESSys simulated streamflow, M m <sup>3</sup>	Deviation from observed, M m <sup>3</sup>	Total RHESSys simulated streamflow, M m <sup>3</sup>	Deviation from observed, M m <sup>3</sup>
ACCESS 1.0	01-04-2016 to 30-09-2016	199.02	183.85	-15.17	222.15	23.13
CCSM 4			202.75	03.72	236.38	37.36
CNRM-CM5			188.36	-10.66	140.04	-58.99
MPI-ESM-LR			198.06	-00.97	192.90	-06.13
NorESM1-M			214.20	15.18	222.12	23.11
Average			197.44	-1.58	202.72	3.70

found to be the most sensitive variables under the RCP 4.5 scenario, whereas saturation deficit and overland flow were found to be the most sensitive variables under the RCP 8.5 scenario.

**Supplementary Information** The online version contains supplementary material available at <https://doi.org/10.1007/s40899-023-00874-7>.

**Acknowledgements** The authors gratefully express their sincere thanks to Central Water Commission (Itanagar) for providing the data for use in this study for hydrological modelling of Nuranang river basin of Tawang district, Arunachal Pradesh.

**Author contributions** PM: conceptualisation, data acquisition, methodology, original draft preparation. AB: supervision, editing of the manuscript. AB: conceptualisation, supervision, editing of the manuscript, visualization.

**Funding** This work is supported by Information Technology Research Academy (ITRA), Government of India under ITRA-Water Grant ITRA/15(69)/Water/M2M/02/2015. The authors also gratefully acknowledge the help, encouragement, and financial support provided by Indo-US Science and Technology Forum (IUSSTF) under Indo-US Research Fellowship and the Climate Change Programme (CCP), Strategic Programmes, Large Initiatives and Coordinated Action Enabler (SPLICE), Department of Science and Technology, Govt. of India under National Mission on Sustaining Himalayan Ecosystem (NMSHE) through Grant No. DST/CCP/MRDP/184/2019.

**Availability of data and material** The discharge data that support the findings of this study are available from Central Water Commission (CWC), India. Restrictions apply to the availability of these data, which

were used under license for this study. These data are available from the authors with the permission of CWC Headquarter, New Delhi. The meteorological data that support the findings of this study are openly available from CWC (precipitation, temperature, and relative humidity). The ASTER DEM data that support the findings of this study are openly available at <https://search.earthdata.nasa.gov/search>. The LULC data that support the findings of this study are available on request from the State Remote Sensing Application Centre, SRSAC, Itanagar. These data are not publicly available due to privacy or ethical restrictions. The soil map data that support the findings of this study are available on request from the State Land Use Board, Arunachal Pradesh. These data are not publicly available due to privacy or ethical restrictions. The CORDEX data used for climate projection are freely downloadable from their website.

**Code availability** The RHESSys modeling system, GRASS GIS, QGIS, and R used in this study are freely available for download. ArcMap is used under license which needs to be procured from ESRI.

## Declarations

**Conflict of interest** The authors declare there is no conflict of interest/competing interest.

**Ethics approval** Not applicable. This article does not contain any studies with human participants or animals.

**Consent to participate** Not applicable.

**Consent for publication** Not applicable.

## References

- Aawar T, Khare D (2020) Assessment of climate change impacts on streamflow through hydrological model using SWAT model: a case study of Afghanistan. *Model Earth Syst Environ* 6:1427–1437. <https://doi.org/10.1007/s40808-020-00759-0>
- Band LE, Patterson P, Nemani R, Running SW (1993) Forest Ecosystem Processes at the Watershed Scale-Incorporating Hillslope Hydrology. *Agric for Meteorol* 63:93–126. [https://doi.org/10.1016/0168-1923\(93\)90024-C](https://doi.org/10.1016/0168-1923(93)90024-C)
- Band LE, Mackay S, Creed IF, Semkin R, Jeffries D (1996) Ecosystem processes at the watershed scale: Sensitivity to potential climate change. *Limnol Oceanogr* 41(5):928–938. <https://doi.org/10.4319/lo.1996.41.5.0928>
- Beaulieu E, Lucas Y, Viville D, Chabaux F, Ackerer P, Godderis Y, Pierret MC (2016) Hydrological and vegetation response to climate change in a forested mountainous catchment. *Model Earth Syst Environ* 2:1–15. <https://doi.org/10.1007/s40808-016-0244-1>
- Beven KJ, Kirkby MJ (1979) A physically based, variable contributing area model of basin hydrology / Un modèle à base physique de zone d'appel variable de l'hydrologie du bassin versant. *Hydrol Sci Bull* 24(1):43–69. <https://doi.org/10.1080/02626667909491834>
- Bhandari R, Kalra A, ZKumar S (2020) Analyzing the Effect of CMIP5 Climate Projections on Streamflow Within the Pajaro River Basin. *Open Water J* 6(1): 5. <https://scholarsarchive.byu.edu/openwater/vol6/iss1/5>.
- Chiew FHS, Teng J, Vaze J, Post DA, Perraud JM, Kirono DGC, Viney NR (2009) Estimating climate change impact on runoff across southeast Australia: Method, results, and implications of the modeling method. *Water Resour Res*. <https://doi.org/10.1029/2008WR007338>
- Dar T, Rai N, Kumar S (2022) Climate change impact on cryosphere and streamflow in the Upper Jhelum River Basin (UJRB) of north-western Himalayas. *Environ Monit Assess* 194:140. <https://doi.org/10.1007/s10661-022-09766-3>
- Dutta P, Hinge G, Marak JDK, Sarma AK (2020) Future climate and its impact on streamflow: a case study of the Brahmaputra river basin. *Model Earth Syst Environ*. <https://doi.org/10.1007/s40808-020-01022-2>
- Etchevers P, Golaz C, Habets F, Noilhan J (2002) Impact of a climate change on the Rhone river catchment hydrology. *J Geophys Res* 107(16):4293. <https://doi.org/10.1029/2001JD000490>
- Fowler HJ, Blenkinsop S, Tebaldi C (2007) Linking climate change modelling to impacts studies: recent advances in downscaling techniques for hydrological modeling. *Int J Climatol* 27:1547–1578. <https://doi.org/10.1002/joc.1556>
- Fung F, Watts G, Lopez A, Orr HG, New M, Extence C (2013) Using large climate ensembles to plan for the hydrological impact of climate change in the freshwater environment. *Water Resour Manag* 27:1063–1084. <https://doi.org/10.1007/s11269-012-0080-7>
- Giorgi F, Jones C, Asrar GR (2009) Addressing climate information needs at the regional level: the CORDEX framework. *World Meteor Organ (WMO). Bulletin* 58(3):175–183. [http://www.wmo.ch/.../index\\_en.html](http://www.wmo.ch/.../index_en.html).
- Hussen B, Mekonnen A, Pingale SM (2018) Integrated water resources management under climate change scenarios in the sub-basin of Abaya-Chamo, Ethiopia. *Model Earth Syst Environ* 4:221–240. <https://doi.org/10.1007/s40808-018-0438-9>
- Maharjan M, Aryal A, Talchabhadel R, Thapa BR (2021) Impact of climate change on the streamflow modulated by changes in precipitation and temperature in the North Latitude Watershed of Nepal. *Hydrology* 8:117. <https://doi.org/10.3390/hydrology8030117>
- Marazi A, Romshoo SA (2018) Streamflow response to shrinking glaciers under changing climate in the Lidder Valley, Kashmir Himalayas. *J Mt Sci* 15(6):1241–1253. <https://doi.org/10.1007/s11629-017-4474-0>
- Martin KL, Hwang T, Vose JM, Coulston JW, Wear DN, Miles B, Band LE (2017) Watershed impacts of climate and land use changes depend on magnitude and land use context. *Ecohydrology* 10(7):1870. <https://doi.org/10.1002/eco.1870>
- Mishra P, Chiphang N, Bandyopadhyay A, Bhadra A (2020) Process-based eco-hydrological modelling in an eastern Himalayan watershed using RHESSys. *Model Earth Syst Environ* 7:2553–2574. <https://doi.org/10.1007/s40808-020-01059-3>
- Morán-Tejeda E, Zabalza J, Rahman K, Gago-Silva A, López-Moreno JI, Vicente-Serrano S, Lehmann A, Tague CL, Beniston M (2015) Hydrological impacts of climate and land-use changes in a mountain watershed: Uncertainty estimation based on model comparison. *Ecohydrology* 8(8):1396–1416. <https://doi.org/10.1002/eco.1590>
- Munawar S, Tahir MN, Baig MHA (2022) Twenty-first century hydrologic and climatic changes over the scarcely gauged Jhelum river basin of Himalayan region using SDSM and RCPs. *Environ Sci Pollut Res* 29(8):11196–11208. <https://doi.org/10.1007/s11356-021-16437-2>
- Pechlivanidis IG, Olsson J, Sharma D, Bosshard T, Sharma KC (2014) Assessment of the Climate Change impact on the water resources of the Luni Region, India. *Global Nest J* 17(1):29–40. <https://doi.org/10.30955/gnj.001370>
- Peng H, Jia YW, Tague C, Slaughter P (2015) An Eco-Hydrological Model-Based Assessment of the Impacts of Soil and Water Conservation Management in the Jinghe River Basin, China. *Water* 7:6301–6320. <https://doi.org/10.3390/w7116301>
- Rani S, Sreekesh S (2019) Evaluating the responses of streamflow under future climate change scenarios in a Western Indian Himalaya Watershed. *Environ Process* 6(1):155–174. <https://doi.org/10.1007/s40710-019-00361-2>
- Romshoo SA, Marazi A (2022) Impact of climate change on snow precipitation and streamflow in the Upper Indus Basin ending twenty-first century. *Clim Change* 170(1):1–20. <https://doi.org/10.1007/s10584-021-03297-5>
- Ruelland D, Ardoin-Bardin S, Collet L, Roucou P (2012) Simulating future trends in hydrological regime of a large SudanoSahelian catchment under climate change. *J Hydrol* 424:207–216. <https://doi.org/10.1016/j.jhydrol.2012.01.002>
- Ruth M, Bernier C, Jollands N, Golubiewski N (2007) Adaptation of urban water supply infrastructure to impacts from climate and socioeconomic changes: the case of Hamilton, New Zealand. *Water Resour Manag* 21(6):1031–1045. <https://doi.org/10.1007/s11269-006-9071-x>
- Sarkar S, Butcher JB, Johnson TE, Clark CM (2018) Simulated sensitivity of urban green infrastructure practices to climate change. *Earth Interact*. <https://doi.org/10.1175/EI-D-17-0015.1>
- Senatore A, Mendicino G, Smiatek G, Kunstmann H (2011) Regional climate change projections and hydrological impact analysis for a Mediterranean basin in Southern Italy. *J Hydrol* 399:70–92. <https://doi.org/10.1016/j.jhydrol.2010.12.035>
- Shiferaw H, Gebremedhin A, Gebretsadkan T, Zenebe A (2018) Modeling hydrological response under climate change scenarios using SWAT model: the case of Ilala watershed, Northern Ethiopia. *Model Earth Syst Environ* 4:437–449. <https://doi.org/10.1007/s40808-018-0439-8>
- Shin H, Park M, Lee J, Lim H, Kim SJ (2019) Evaluation of the effects of climate change on forest watershed hydroecology using the RHESSys model: Seolmacheon catchment. *Paddy Water Environ* 17:581–595. <https://doi.org/10.1007/s10333-018-00683-1>
- Singh V, Jain SK, Goyal MK (2021) An assessment of snow-glacier melt runoff under climate change scenarios in the Himalayan

- basin. *Stoch Environ Res Risk Assess* 35:2067–2092. <https://doi.org/10.1007/s00477-021-01987-1>
- Singh O, Sharma MC (2022) Variability and trends in temperature, rainfall, and discharge In a Western Himalayan catchment. In: *Climate change*, Springer climate, Springer, pp 29–45. [https://doi.org/10.1007/978-3-030-92782-0\\_2](https://doi.org/10.1007/978-3-030-92782-0_2)
- Son K, Tague C (2018) Hydrologic responses to climate warming for a snow-dominated watershed and a transient snow watershed in the California Sierra. *Ecohydrology* 12(1):2053. <https://doi.org/10.1002/eco.2053>
- Tague CL, Band LE (2004) RHESSys: Regional Hydro-Ecologic Simulation System-An Object-Oriented Approach to Spatially Distributed Modeling of Carbon, Water, and Nutrient Cycling. *Earth Interact* 8(19):1–42. [https://doi.org/10.1175/1087-3562\(2004\)8%3c1:RRHSSO%3e2.0.CO;2](https://doi.org/10.1175/1087-3562(2004)8%3c1:RRHSSO%3e2.0.CO;2)
- Tarekegn N, Abate B, Muluneh A, Dile Y (2021) Modeling the impact of climate change on the hydrology of Andasa watershed. *Model Earth Syst Environ* 8:103–119. <https://doi.org/10.1007/s40808-020-01063-7>
- Thapa S, Li H, Li B, Fu D, Shi X, Yabo S, Lu L, Qi H, Zhang W (2021) Impact of climate change on snowmelt runoff in a Himalayan basin. *Nepal Environ Monit Assess* 193:393. <https://doi.org/10.1007/s10661-021-09197-6>
- Thiha S, Shamseldin AY, Melville BW (2020) Assessment of the Myitnge River flow responses in Myanmar under changes in land use and climate. *Model Earth Syst Environ*. <https://doi.org/10.1007/s40808-020-00926-3>
- Tiwari S, Kar SC, Bhatla R (2018) Mid-21st century projections of hydroclimate in western Himalayas and Satluj River basin. *Glob Planet Change* 161:10–27. <https://doi.org/10.1016/j.gloplacha.2017.10.013>
- Urrutia R, Vuille M (2009) Climate change projections for the tropical Andes using a regional climate model: Temperature and precipitation simulations for the end of the 21st century. *J Geophys Res*. <https://doi.org/10.1029/2008JD011021>
- Wigmosta MS, Vail LW, Lettenmaier DP (1994) A distributed hydrology-vegetation model for complex terrain. *Water Resour Res* 30(6):1665–1679. <https://doi.org/10.1029/94WR00436>
- Wolock DM (1993) Simulating the variable-source-area concept of streamflow generation with the watershed model TOPMODEL. U.S. Geological Survey, Water Resources Division Water-Resources Investigations Report 93-4124. <https://doi.org/10.3133/wri934124>
- Zabalza-Martínez J, Vicente-Serrano S, López-Moreno J, Borràs Calvo G, Savé R, Pascual D, Pla E, Morán-Tejeda E, Domínguez-Castro F, Tague CL (2018) The influence of climate and land-cover scenarios on dam management strategies in a high water pressure catchment in Northeast Spain. *Water* 10(11):1668. <https://doi.org/10.3390/w10111668>

**Publisher's Note** Springer Nature remains neutral with regard to jurisdictional claims in published maps and institutional affiliations.

Springer Nature or its licensor (e.g. a society or other partner) holds exclusive rights to this article under a publishing agreement with the author(s) or other rightsholder(s); author self-archiving of the accepted manuscript version of this article is solely governed by the terms of such publishing agreement and applicable law.